Sohm Abyssal Plain: Evaluating Proximal Sediment Provenance

DANIEL JEAN STANLEY, PATRICK T. TAYLOR,
HARRISON SHENG, and ROBERT STUCKENRATH

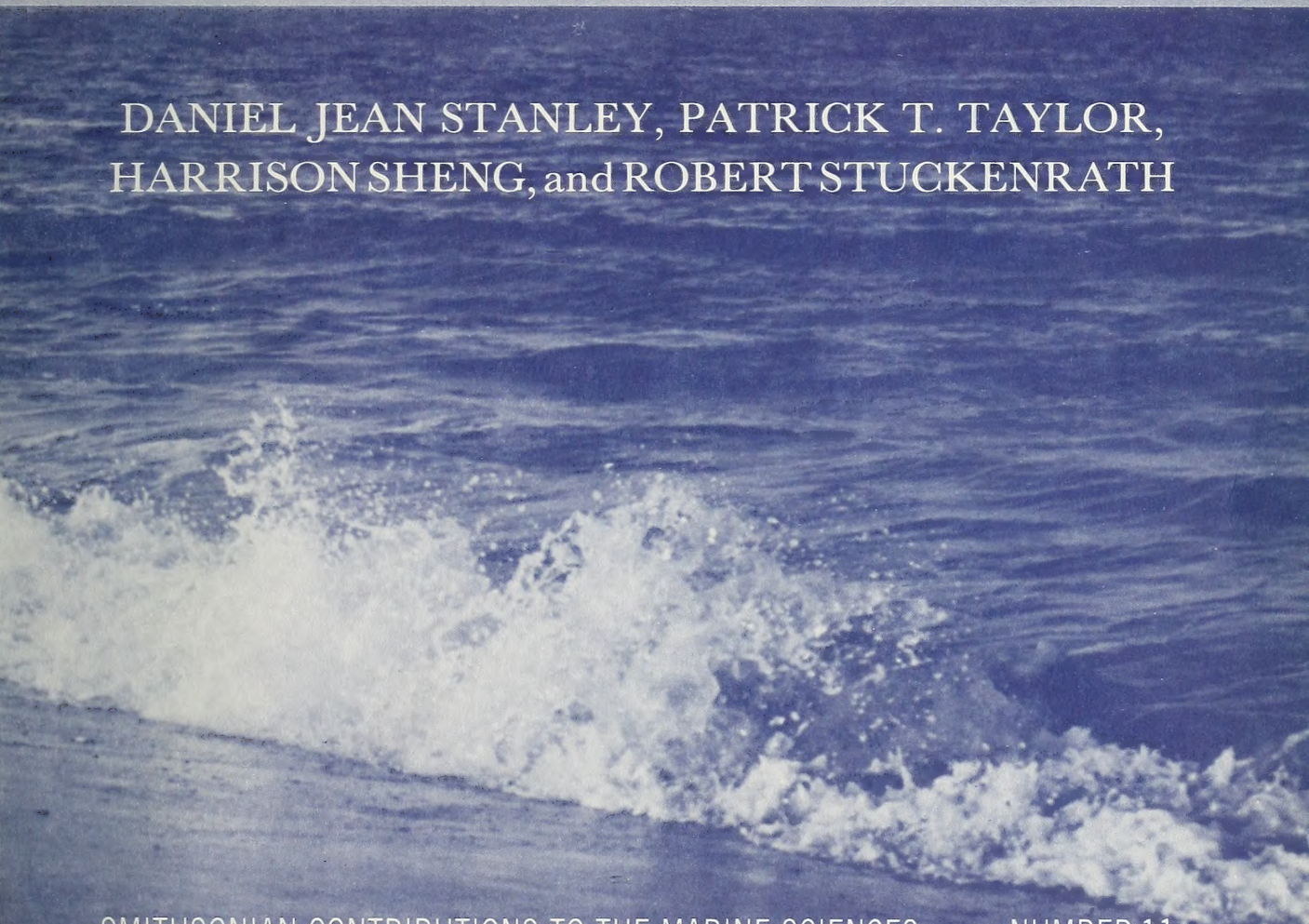

SMITHSONIAN CONTRIBUTIONS TO THE MARINE SCIENCES • NUMBER 11

SERIES PUBLICATIONS OF THE SMITHSONIAN INSTITUTION

Emphasis upon publication as a means of "diffusing knowledge" was expressed by the first Secretary of the Smithsonian. In his formal plan for the Institution, Joseph Henry outlined a program that included the following statement: "It is proposed to publish a series of reports, giving an account of the new discoveries in science, and of the changes made from year to year in all branches of knowledge." This theme of basic research has been adhered to through the years by thousands of titles issued in series publications under the Smithsonian imprint, commencing with *Smithsonian Contributions to Knowledge* in 1848 and continuing with the following active series:

Smithsonian Contributions to Anthropology
Smithsonian Contributions to Astrophysics
Smithsonian Contributions to Botany
Smithsonian Contributions to the Earth Sciences
Smithsonian Contributions to the Marine Sciences
Smithsonian Contributions to Paleobiology
Smithsonian Contributions to Zoology
Smithsonian Studies in Air and Space
Smithsonian Studies in History and Technology

In these series, the Institution publishes small papers and full-scale monographs that report the research and collections of its various museums and bureaux or of professional colleagues in the world of science and scholarship. The publications are distributed by mailing lists to libraries, universities, and similar institutions throughout the world.

Papers or monographs submitted for series publication are received by the Smithsonian Institution Press, subject to its own review for format and style, only through departments of the various Smithsonian museums or bureaux, where the manuscripts are given substantive review. Press requirements for manuscript and art preparation are outlined on the inside back cover.

S. Dillon Ripley
Secretary
Smithsonian Institution

SMITHSONIAN CONTRIBUTIONS TO THE MARINE SCIENCES • NUMBER 11

Sohm Abyssal Plain: Evaluating Proximal Sediment Provenance

Daniel Jean Stanley, Patrick T. Taylor, Harrison Sheng, and Robert Stuckenrath

SMITHSONIAN INSTITUTION PRESS
City of Washington
1981

ABSTRACT

Stanley, Daniel Jean, Patrick T. Taylor, Harrison Sheng, and Robert Stuckenrath. Sohm Abyssal Plain: Evaluating Proximal Sediment Provenance. *Smithsonian Contributions to the Marine Sciences*, number 11, 48 pages, 23 figures, 5 tables, 1981.—The southernmost part of the Sohm Abyssal Plain in the Northwest Atlantic Basin is geographically distal with respect to the major source of Quaternary terrigenous material transported from the Canadian Maritime Provinces. An assessment of the proportion of more locally introduced sediment relative to that derived from distal sources is based largely on size and compositional analyses of Quaternary piston core samples. These data are supplemented by radiocarbon dating of selected core samples, bottom photographs, conductivity-temperature-depth profiles, and seismic records.

The premises of the study are that (a) locally derived sediment should be most abundant near high-relief bathymetric features such as seamounts and abyssal hills, and (b) such material should contain enhanced proportions of reworked volcanic debris and alteration products. Core analyses reveal that the amounts of these are directly related to proximity of volcanic ocean-bottom features, and that a significant, although not total, amount of such volcanic materials recovered from cores are derived from submarine weathering of basalt. Associated with this assemblage are nannofossils, dating from the Quaternary to the Upper Cretaceous, reworked from older strata. This increased proportion of volcanic and related products and reworked faunas near seamounts and basement rises strongly implies that such topographic features continue to serve as major source terrains. Locally derived volcanic materials, however, are usually disseminated and masked on the Sohm Abyssal Plain, particularly in sectors receiving large amounts of terrigenous turbidites and biogenic suspensates, and/or undergoing reworking by bottom currents.

We propose that the volcanic fraction can serve as a useful index, or "yardstick," to interpret the role of locally derived material in abyssal plain sedimentation. A sedimentation model is developed to illustrate the premise that as access to land-derived sources diminishes, the proportion of terrigenous components is reduced while pelagic and volcanic fractions are enhanced. Thus, sediment accumulating in abyssal plains almost totally isolated from terrigenous sources would comprise significant amounts of pelagic (including wind-blown) and volcanic components. Our model illustrates that even in an abyssal plain, such as the Sohm, which has had an important and direct access to abundant distally derived terrigenous sources, particularly during the Pliocene and Quaternary, the locally supplied reworked volcanic products account for a significant fraction of the total abyssal plain sediment fill.

OFFICIAL PUBLICATION DATE is handstamped in a limited number of initial copies and is recorded in the Institution's annual report, *Smithsonian Year*. SERIES COVER DESIGN: Seascape along the Atlantic coast of Eastern North America.

Library of Congress Cataloging in Publication Data
Sohm Abyssal Plain
(Smithsonian contributions to the marine sciences ; 11)
Bibliography: p.
1. Marine sediments—Sohm Plain (Atlantic Ocean) I. Stanley, Daniel J. II. Series: Smithsonian Institution. Smithsonian contributions to the marine sciences ; no. 11.
GC383.S64 551.46'4 81-607056 AACR2

Contents

Sohm Abyssal Plain: Evaluating Proximal Sediment Provenance

Daniel Jean Stanley, Patrick T. Taylor, Harrison Sheng, and Robert Stuckenrath

Introduction

Following the classic work of Heezen and Ewing (1952), studies of North Atlantic abyssal plains during the past three decades have emphasized turbidity currents as a major transporting agent in the displacement of sediment to remote regions. This process has been proposed largely as a result of piston core investigations which show that surficial Atlantic sequences commonly contain a sand fraction comprising clastic, shallow-marine or land-derived components (Ericson et al., 1961; Heezen, 1963; Horn et al., 1971). The acoustic patterns on seismic reflection profiles of the Northwest Atlantic Basin show multiple returns (termed acoustically layered) that are generally interpreted as stacked sequences of turbidites (Ewing et al., 1973). Seismic surveys in this region also indicate the presence of transparent acoustic series, primarily on topographic highs, which are believed to have a different origin (Ewing et al., 1973; Bowles, 1980). Interpretations of acoustically transparent layers are based on JOIDES deep-sea drilling results, bottom photography (Heezen and Hollister, 1971), nephelometry (Biscaye and Eittreim, 1977), and studies of water-mass motion (Laine, 1978). Various transport models, for the most part involving resuspension by bottom currents, have evolved from these investigations.

Recent reassessment of the origin of sediments in the Northwest Atlantic Basin, including the large, deep (>5000 m), T-shaped Sohm Abyssal Plain south of the Canadian Maritime Provinces (Heezen and Tharp, 1968), indicates an even more complex depositional origin (Figure 1). Biscaye and Eittreim (1977) summarize the importance of concentrated suspended material in the water masses on and above this Plain, and attribute the almost ubiquitous bottom-hugging nepheloid layer to erosion and resuspension of the seafloor by bottom-water flow. Amos and Gerard (1979), however, suggest that a nepheloid layer in the northern sector of the Sohm Plain is due to material carried southward by a transport process related to turbidity currents. The discovery of a large clockwise-circulating gyre associated with the Gulf Stream System (Worthington, 1976) has led to a modification of the classic turbidite and nepheloid layer emplacement models for this area. According to Laine and Hollister (1981), flow associated with this gyre resuspends seafloor sediment and also entrains turbidity current flows periodically introduced into the Sohm Abyssal Plain from the Canadian Maritime Margin.

All the above sedimentation schemes, and com-

Daniel Jean Stanley and Harrison Sheng, Division of Sedimentology, Smithsonian Institution, Washington, D.C. 20560; Patrick T. Taylor, Earth Survey Applications Division, NASA Goddard Space Flight Center, Greenbelt, Md. 20771; and Robert Stuckenrath, Radiation Biology Laboratory, Smithsonian Institution, Washington, D.C. 20560.

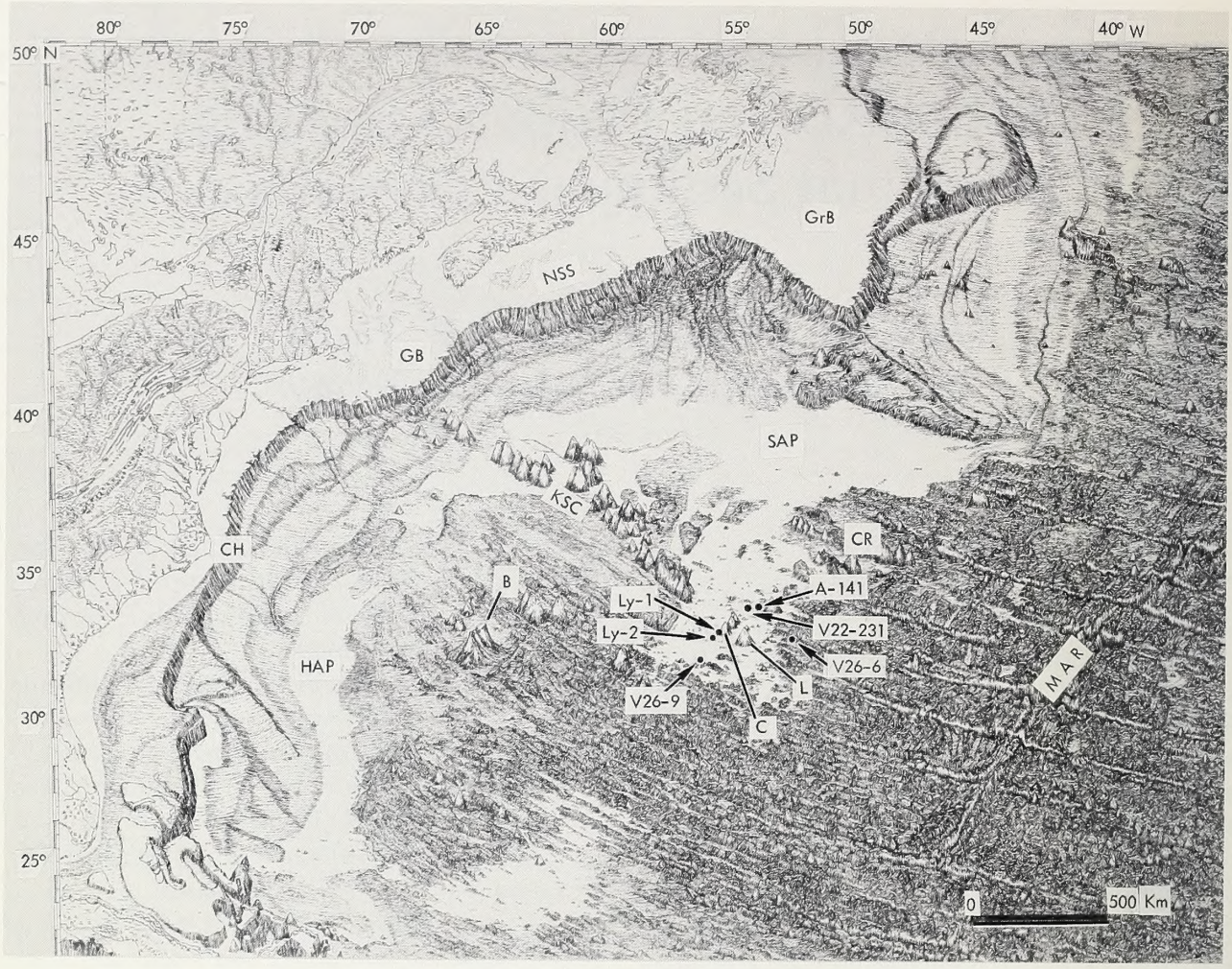

FIGURE 1.—Chart of Northwest Atlantic Basin (abbreviations for features cited in text: GrB = Grand Banks, NSS = Nova Scotian Shelf, GB = Georges Bank, CH = Cape Hatteras, HAP = Hatteras Abyssal Plain, SAP = Sohm Abyssal Plain, KSC = Kelvin Seamount Chain, MAR = Mid-Atlantic Ridge, CR = Corner Rise, B = Bermuda; C = Congress Seamount, L = Lynch Seamount; core locations: Ly = *Lynch* 710-78 cores, A = *Atlantis* 153 core, V = *Vema* 22 and 26 cores).

binations thereof, are generally applicable on a basin-wide scale and tend to emphasize remote provenance and long-distance dispersal of terrigenous and biogenic material by near-bottom current activity. There has been a tendency, however, to overlook the contribution of locally derived material in regional depositional interpretations. In order to focus more precisely on this potentially important aspect, we selected for study the southernmost part of the Sohm Abyssal Plain. This area represents a geographically distal sector with respect to the major source of the Quaternary terrigenous material transported onto the plain, i.e., the Canadian Maritime Margin (Horn et al., 1971). Thus, our study will attempt to assess the proportion of more locally introduced sediment relative to that derived from distal sources. It could be assumed that the amount of locally derived sediment should be higher in cores recovered from this remote region than those collected in more proximal areas.

The southern sector of the Sohm Abyssal Plain is bordered on three sides by abyssal hills of low to moderate relief (Heezen et al., 1959; Horn et al., 1971). Samples and seismic data were collected near the center of this region, specifically around Congress and Lynch seamounts, isolated bathymetric highs in this region (Figures 1 and 2). These data supplement more widely spaced geological and geophysical measurements previously collected by others—principally from the Lamont-Doherty Geological Observatory (L-DGO)—in the plain (Ewing et al., 1974:138, 229). Our working premises for this study are (a) that locally derived sediment should be most abundant near high-relief bathymetric features (e.g., seamounts, ridges, and large abyssal hills), and (b) that such material should contain enhanced proportions of volcanic debris. To test this idea,

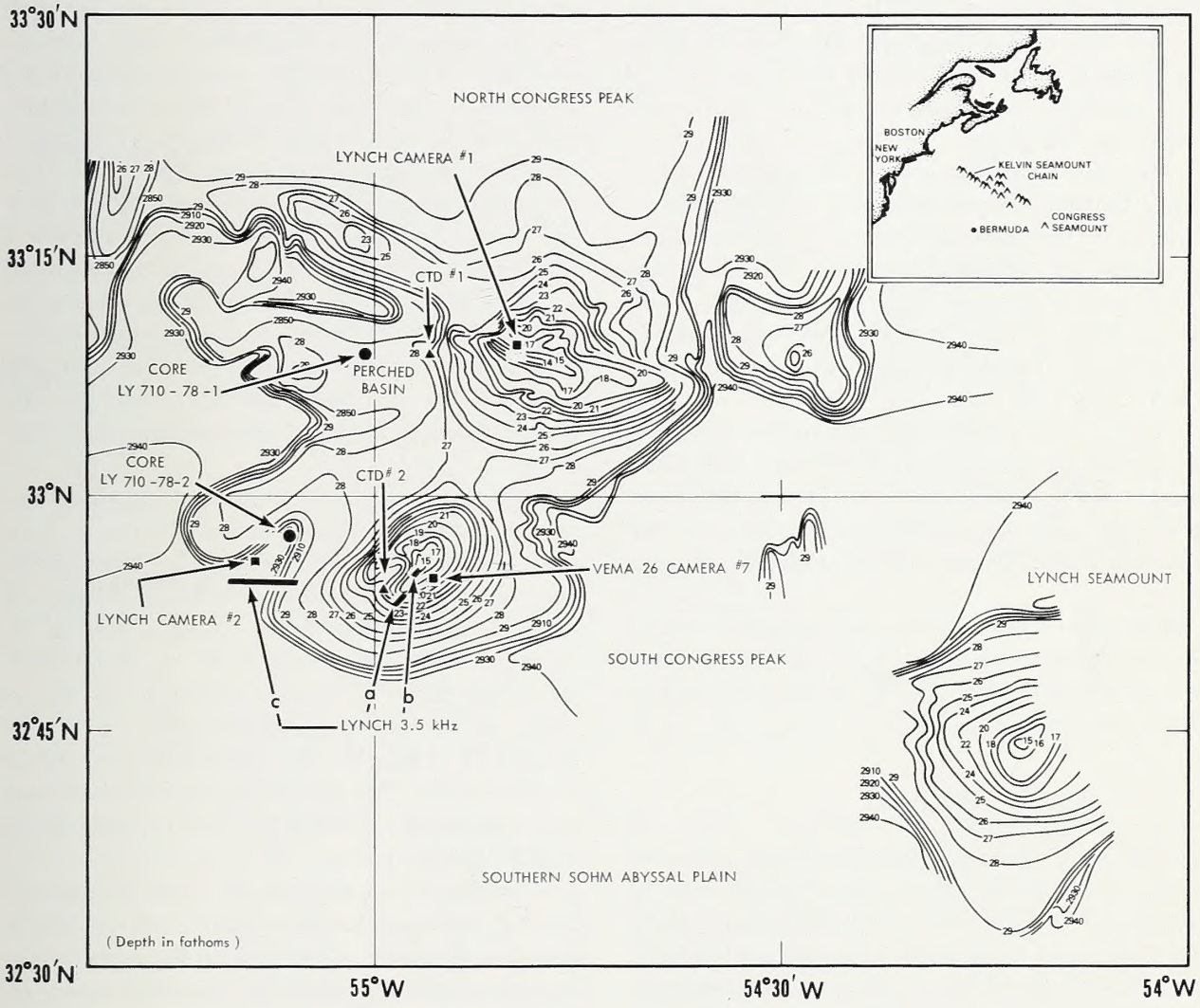

FIGURE 2.—Sampling stations around the Congress and Lynch seamounts in the Southern Sohm Abyssal Plain; note the perched basin on western flank of the Congress seamount (bathymetry from *Lynch* cruise 710-78 in 1978; solid circles = core stations, squares = camera stations; triangles = CTD stations, solid bars (a, b, c) = 3.5 kHz profiles, shown also, in part, in Figure 10; depths shallower than 2910 fathoms given in hundreds of fathoms).

six cores recovered on or within 220 km (120 nm) of Congress Seamount (Figure 1) were examined: two each near the Congress, on the southern Abyssal Plain proper, and on the somewhat higher relief volcanic topography peripheral to the plain.

ACKNOWLEDGMENTS.—We thank the U.S. Navy for supporting cruise 710-78 of the USNS *Lynch* and, particularly, Capt. John T. Lawrence, the officers, crew, and scientific party who ably assisted in the work at sea. Dr. David Greenewalt, Naval Research Laboratory, Washington, D.C., provided us with preliminary interpretations of the conductivity-temperature-depth data collected on this cruise.

We have benefited greatly from access to the core, bottom photograph, and seismic data libraries of the Lamont-Doherty Geological Observatory of Columbia University, Palisades, New York, and are grateful to Drs. F. W. McCoy and W. Ludwig, and to Ms. B. Batchelder and Mr. L. Sullivan for their help in providing us with data used in this study.

Appreciation is also expressed to Drs. S. Streeter, Lamont-Doherty, and C. C. Smith, U.S. Geological Survey, Washington, D.C., for identification and assistance in the interpretation of the benthic foraminifera and nannofossils, respectively.

The paper has been reviewed by L. A. Barnard, Texas A & M University, T.-C. Huang, University of Rhode Island, and G. H. Keller, Oregon State University.

Methods

The Congress and Lynch seamounts were surveyed by the USNS *Lynch* (cruise 710-78) from 30 September to 6 October 1978. Bathymetric data were obtained in fathoms with the *Lynch's* hull-mounted 12 kHz echo-sounding system and contoured in these units; the uncorrected contours shown in Figures 2 and 3 incorporate previous hydrographic ship crossings of this feature (data obtained from the Defense Mapping Agency, Hydrographic Topographic Center Data Library, Brookmount, Maryland). Throughout the text of this paper, depths and other units are given in metric units; in most instances, equivalent English units are presented for convenience. Seismic reflection profiler data (36 kiloJoule sparker system) collected during the *Lynch* cruise were supplemented by airgun (25 cu in, or 0.4 m^3) records obtained during *Vema* cruises 22 and 26 (8 June 1966 and 8 August 1968, Ewing et al., 1974:138, 229). The more than 1000 line-kilometers of *Lynch* reflection data include 554 km in an east-west direction and 482 in north-south and diagonal directions (Figure 3). Line spacing around the Congress ranges from 3 to 10 km. *Lynch* subbottom 3.5 kHz profiles also were obtained adjacent to and on the mount proper, in the vicinity of the two conductivity-temperature-depth (CTD) profiles shown in Figure 2. At these CTD stations a Neil Brown instrument (Brown, 1974) was used. The first station (33°09′N, 54°58′W) was on the western flank of the northern Congress peak some three kilometers east of *Lynch* core 710-78-1; the second CTD (32°56′N, 54°57′W) was on the western flank of the southern Congress peak (Figure 2).

Seafloor photographs were taken at three stations on and near the Congress (Figure 2). Two stations were occupied during the *Lynch* cruise and one station on *Vema* cruise 26. These are situated as follows: *Lynch* camera station 1, 33°09′N, 54°50′W, 3110–3290 m (1700–1800 fm); *Vema* cruise 26, camera station 7 (13 August 1968), on the southern Congress peak, 32°55.2′N, 54°55.6′W, 2850–2815 m (1560–1540 fm); *Lynch* camera station 2 on the Sohm Abyssal Plain west of the seamount, 32°56′N, 55°12.5′W, about 5367 m (2935 fm).

Two piston cores were obtained during the *Lynch* cruise from the immediate vicinity of the Congress (Figure 2): core *Ly* 710-78-1, taken near the base of the seamount in a perched basin (or pond) near the point of thickest sediment accumulation about 20 km west of the northern Congress peak, is 558 cm long (33°09.3′N, 55°00.2′W, 5207 m, or 2847 fm, depth); core *Ly* 710-78-2, from the adjacent plain, returned only a few

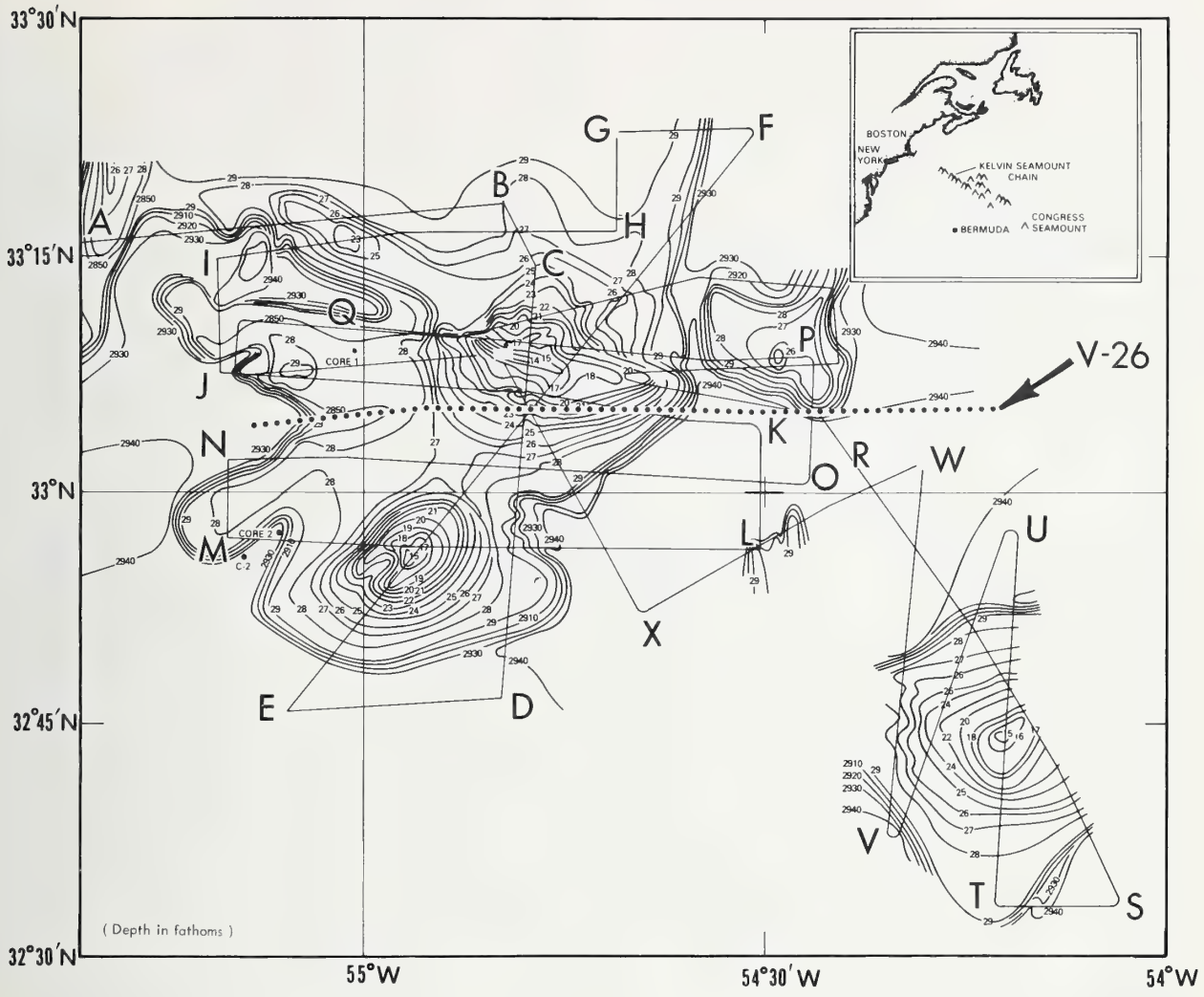

FIGURE 3.—Chart showing location of continuous seismic sparker profiles made on *Lynch* cruise 710-78 (selected records, bounded by points A through X, shown in Figures 5–9; dotted line denotes airgun profile from *Vema* cruise 26, shown in Figures 4A and 13; depths shallower than 2910 fathoms given in hundreds of fathoms).

centimeters of surficial sediment due to pretripping of the piston in the core barrel (32°57.3′N, 55°06.6′W, 5359 m, or 2930 fm, depth). These materials were supplemented by four L-DGO cores (for locations see Figure 1 and also Horn et al., 1971, their fig. 5). Two are located on the plain proper, northeast of the seamount: R/V *Atlantis* core 153-141 (33°26.5′N, 53°48′W; 5350 m, or 2925 fm, depth; 1025 cm core length; also described by Ericson et al., 1961), and R/V *Vema* core 22-231 (33°29′N, 54°10′W; 5535 m, or 3026 fm, depth; 1507 cm core length). A third is located on the surrounding abyssal hills to the east of the southern plain: R/V *Vema* core 26-6 (32°42′N, 52°36′W; 5207 m, or 2847 fm, depth; 587 cm core length). The fourth was recovered on the southernmost fringe of the plain southwest of the Congress: R/V *Vema* core 26-9 (31°43′N, 56°12′W; 5546 m, 3032 fm, depth; 609 cm core length).

The lithofacies of the cores are based on visual observations of split cores; only *Lynch* core 710-

78-1 was x-radiographed. Core analyses also included textural measurements (percentages by weight of sand, silt, and clay fractions); these data are presented in Table 1. Compositional descriptions were made on a total of 75 samples taken from the 5 cores and presented in Tables 2 to 5. Mineralogical studies included the following: (1) estimated proportions of components of sand and coarse silt (>15 μm) sizes (Table 1) using petrographic (transmitted and reflected light) and binocular microscopes; (2) x-ray diffraction of the clay and silt fractions; (3) x-ray fluorescence

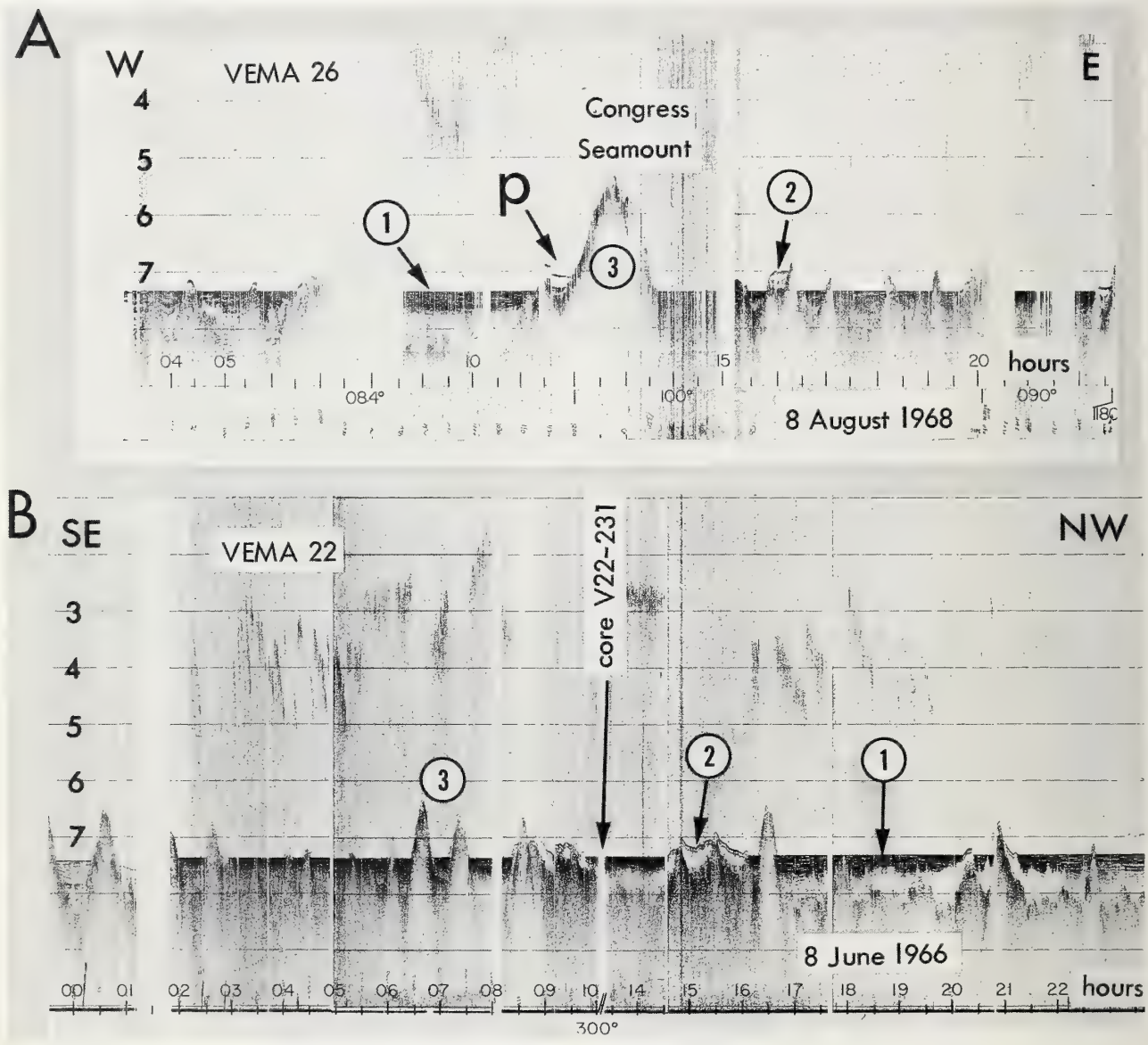

FIGURE 4.—Selected airgun profiles from *Vema* cruises 26 and 22 (profiles A and B, respectively) across the southern Sohm Abyssal Plain in, and in the vicinity of, our study area (from Ewing et al., 1974), showing examples of different acoustic seismic patterns: (1) acoustically layered, (2) acoustically transparent, (3) opaque (basement); note the perched basin (p) on the western flank of the Congress Seamount (vertical scale denotes seconds of two-way travel time; horizontal scale expressed in hours; speed estimated at 9 knots, or 17 km per hour).

(counts per 0.1 mg of sample per 200 seconds) of selected sand, silt, and clay samples; and (4) Scanning Electron Microscope (SEM, Cambridge MKIIA) and electron probe energy dispersive analysis (Tracor Northern Energy Dispersive Spectrometer) of selected silt and fine sand grains. Radiocarbon dates were determined for *Lynch* core 710-78-1 (5 successful dates), and from *Vema* core 22-231 (2 successful dates).

Physiography of Study Area

The Sohm Abyssal Plain, covering an area of about 660,000 km^2, is a T-shaped province situated south of Georges Bank, Nova Scotian Shelf, and Grand Banks (Heezen et al., 1959). The southern portion of the vertical bar of the T extends about 780 km (420 nm) south of the Maritime Continental Margin and lies east of Bermuda (Figure 1). Abyssal depths range from 5120 m (2800 fm) to 5670 m (3100 fm). Bathymetric detail in the study area, between 31° and 34°N latitude and bisected by the 55°W meridian, remains poorly defined. Two large seamounts, the Congress and the Lynch, are located in the approximate center of this sector of the plain (Figure 1). Results from widely spaced seismic profiles across this region are summarized by Ewing et al. (1973). The southern Sohm Plain is not a featureless region as has been generally depicted. Typical airgun profiles across the area show the near-horizontal plain broken by numerous topographic features of highly variable size and relief. Flat monotonous stretches of plain are generally less than 50 km wide between these highs (Figure 4).

Congress Seamount (33°07′N, 54°50′W), located at the distal southeast end of the Kelvin Seamount chain, some 1114 km (600 nm) due east of Bermuda (Figure 2), was first charted by the United States Hydrographic Survey ship USS *Congress* in 1910. Its nearest large neighbors are the Wyoming and Nashville seamounts, about 150 and 210 km to the northwest (Tucholke and Vogt, 1979), and a previously unnamed mount, herein referred to as the Lynch Seamount, approximately 90 km to the southeast (Figure 2).

Congress is a twin-peaked seamount (Figures 2, 3, and 5, profile E–F). The NE–SW trending peaks, separated by 27 km (15 nm), lie at approximately the same depth; the northern summit is slightly shallower (2554 m, 1397 fm) than the southern peak (2578 m, 1410 fm). They rise 2803 m (1533 fm) and 2779 m (1520 fm), respectively, above the floor of the surrounding Sohm Abyssal Plain (5357 m, 2930 fm). The average overall slope of the northern peak is approximately 9°; the slope increases toward the summit (13°), and diminishes near the base (<3°). The average slope of the southern peak is about 10°, the near-summit slope is 16°, and the basal slope <4°.

The depth of the Sohm Abyssal Plain around the Lynch and Congress seamounts is approximately the same. The relief of the Lynch Seamount (2642 m, 1445 fm), however, is somewhat less than that of the Congress inasmuch as the Lynch peak is about 179 m (98 fm) deeper. The basal area of the single-peaked Lynch mount is comparable in size to that of either of the Congress peaks (Figure 6).

One area of the Congress Seamount selected for detailed study is the perched basin between the western flank of the northern peak and a topographic ridge just to the west (Figure 2 and Figure 7, profile J–K). The surface of this depression lies at about 4882 m (2870 fm), or about 475 m (260 fm) above the Sohm Abyssal Plain. The maximum dimensions of this perched, bean-shaped depression are 30 km in an E–W direction and about 29 km in a N–S direction; its approximate surface area is 450 km^2 (Figure 2).

Sediment Acoustic Facies in Southern Plain

General Distribution.—The closely spaced grid of *Lynch* seismic profiles near the Congress and Lynch seamounts (Figure 3) provides the means to define the distribution of two types of unconsolidated sediment in the center of the southern Sohm Plain study area. The survey reveals the configuration of (a) flat-lying, acoust-

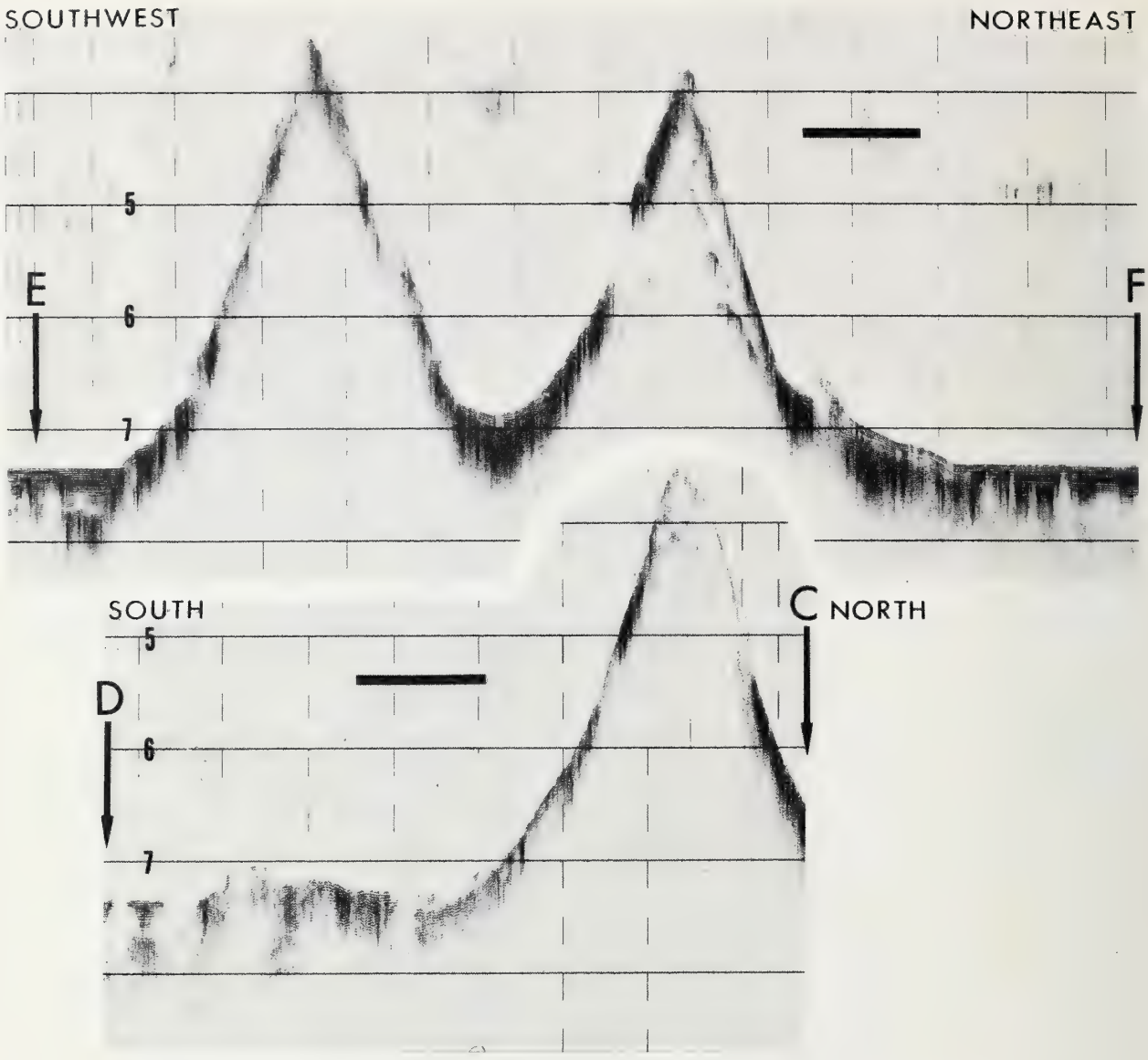

FIGURE 5.—Seismic profiles (30 kJ sparker) showing the twin peaks of Congress Seamount (profile E–F); note the flat-lying, acoustically layered facies forming the Sohm Abyssal Plain and acoustically transparent pattern in the saddle between two peaks (profile C–D) (letters refer to *Lynch* track lines in Figure 3; heavy horizontal bar represents 10 km; vertical scale given in seconds of two-way travel time from the surface).

ically layered sediment, representing the most common reflection pattern in the plain surrounding the seamounts (Figure 4, pattern 1; Figure 7, profiles D–E and L–M; and Figure 8), and (b) the more localized, acoustically transparent pattern (Figure 4, pattern 2; Figure 7, profiles J–K, P–Q, and N–O; and Figure 9). An acoustically opaque series forms the seamount structure, and possible some volcaniclastic apron sediment (Figure 4, pattern 3; and Figures 5 and 6). This opaque pattern underlies either the acoustically layered or transparent layer, or both (Figure 7, profile N–O). The acoustically layered series occurs at depths greater than 5360 m (2930 fm).

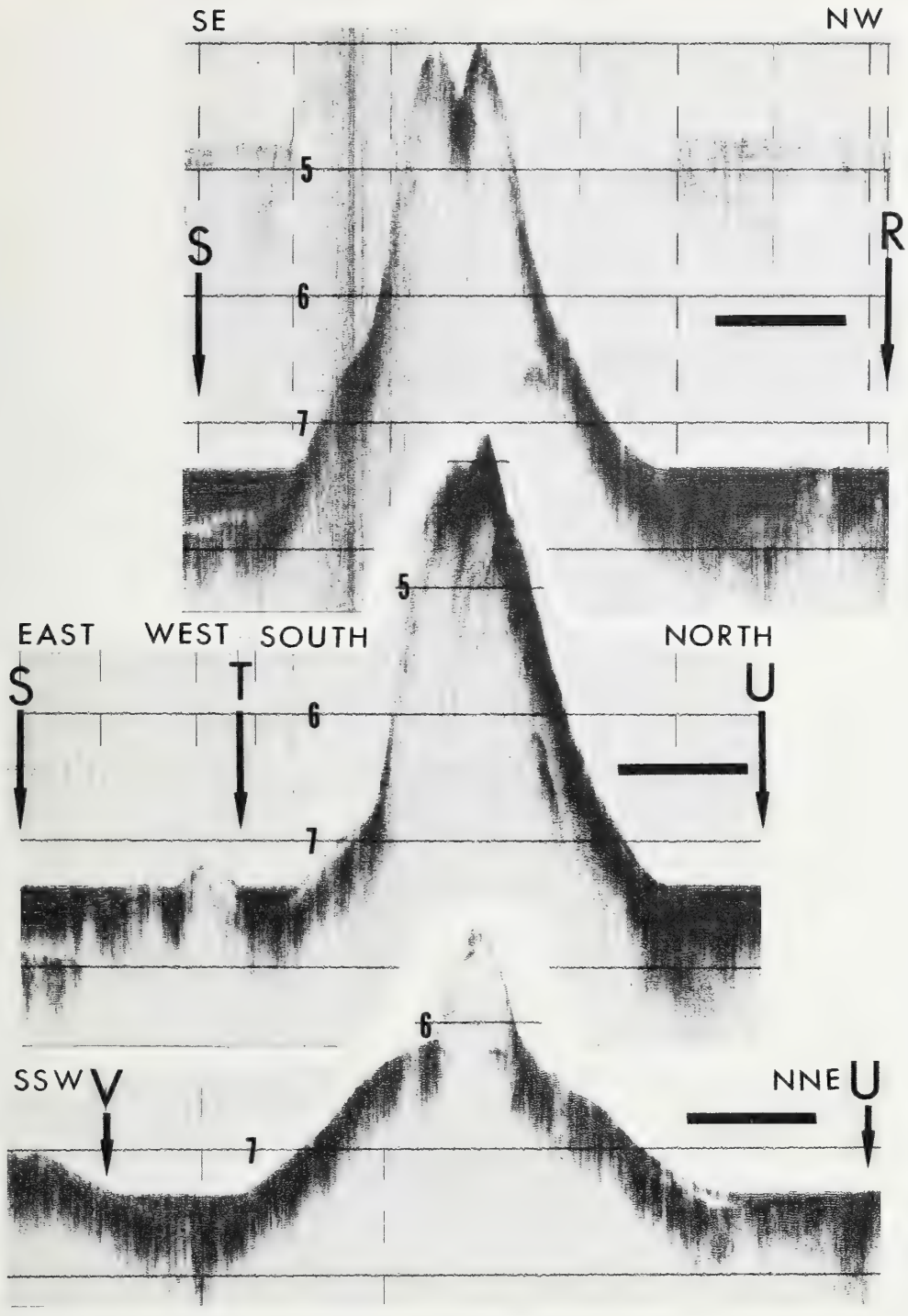

FIGURE 6.—Seismic profiles showing the single-peaked Lynch Seamount; note crater-like depression on peak (profile R–S), acoustically transparent pattern localized on southern flank (profile T–U), and acoustically layered abyssal plain facies (profile U–V); sharp peak on profile U–V may be a side echo (for other explanations see legend for Figure 5).

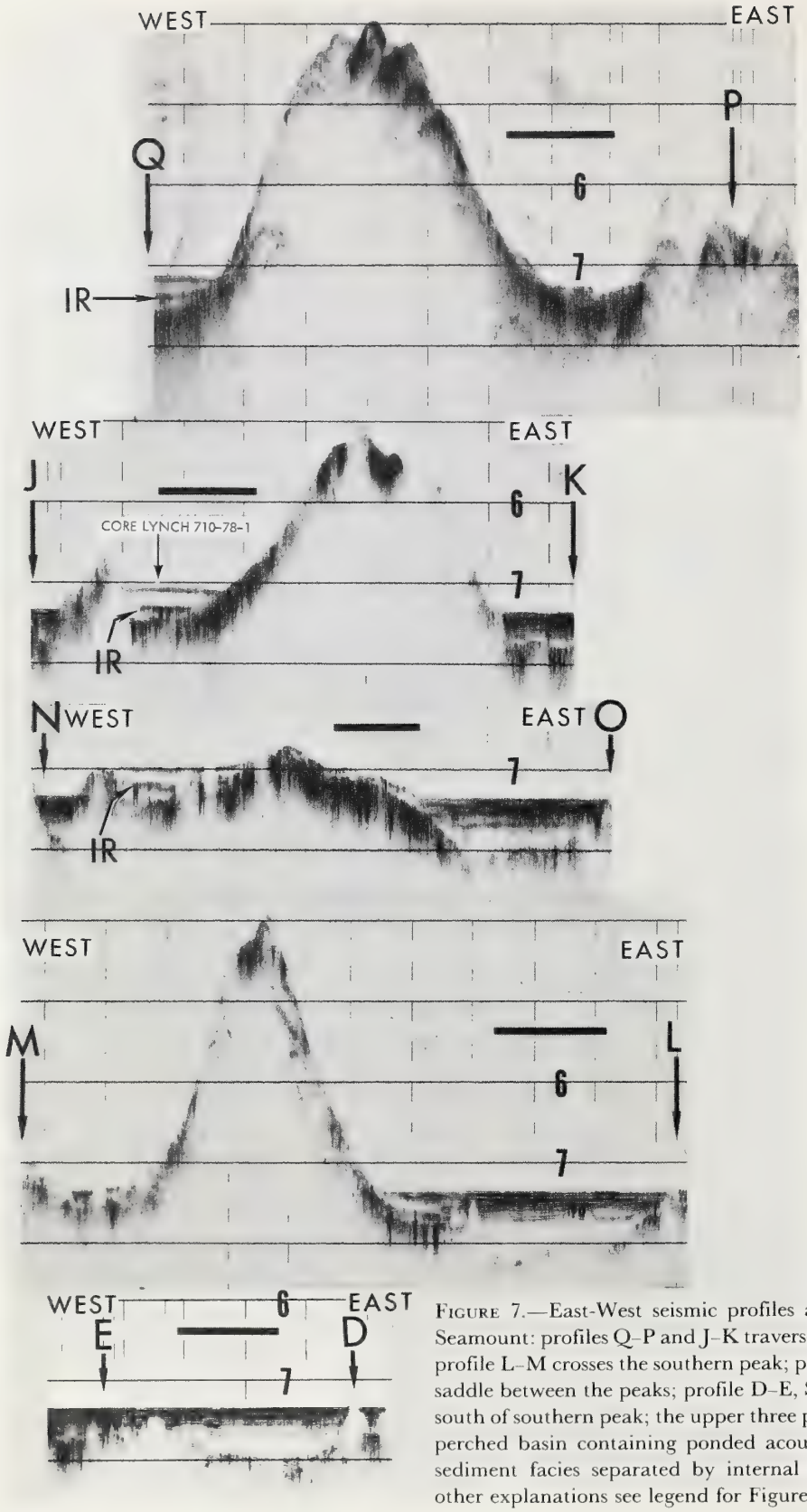

FIGURE 7.—East-West seismic profiles across the Congress Seamount: profiles Q–P and J–K traverse the northern peak; profile L–M crosses the southern peak; profile N–O traverses saddle between the peaks; profile D–E, Sohm Abyssal Plain south of southern peak; the upper three profiles illustrate the perched basin containing ponded acoustically transparent sediment facies separated by internal reflectors (IR) (for other explanations see legend for Figure 5).

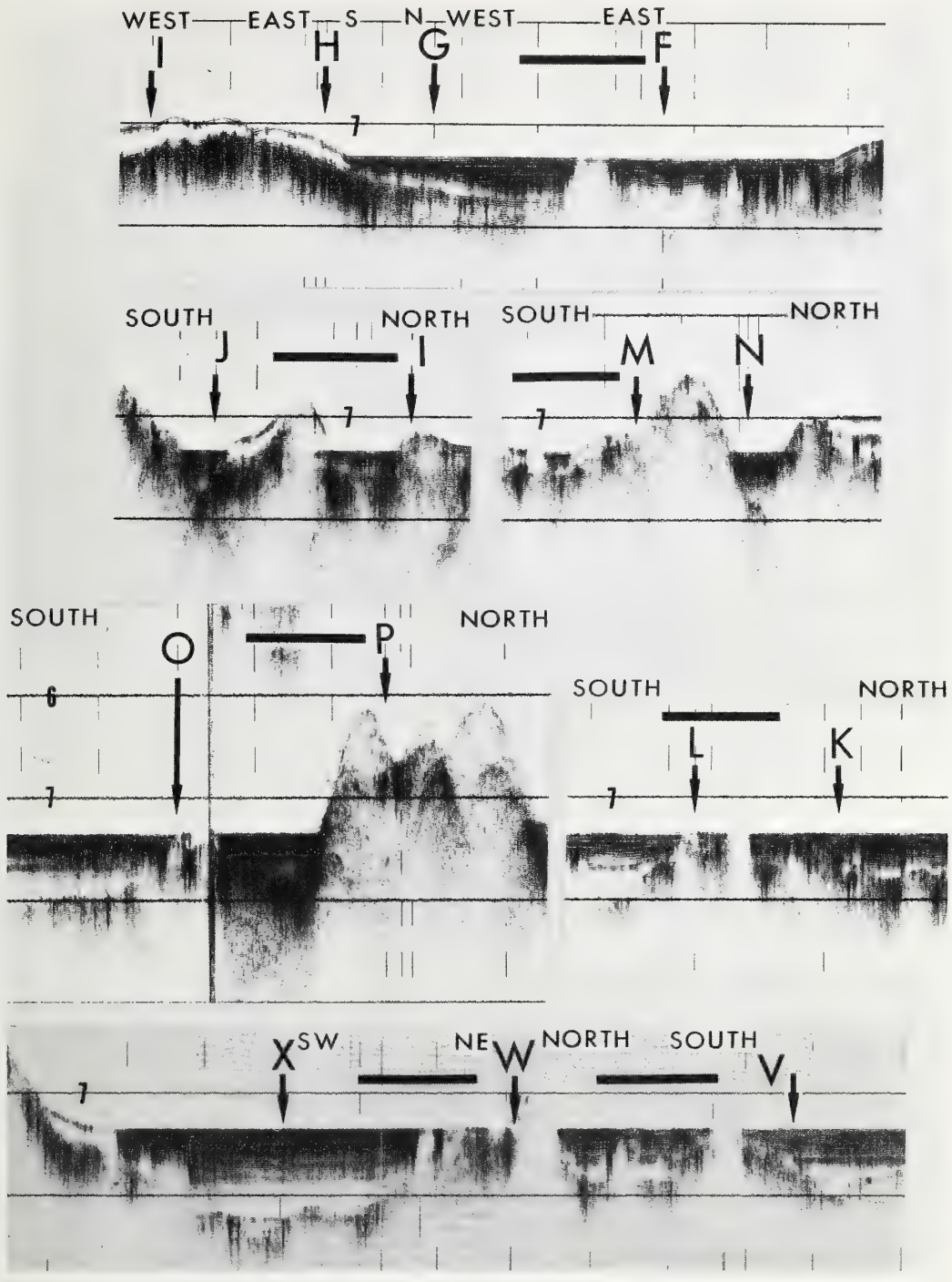

FIGURE 8.—Seismic profiles showing the acoustically layered reflection pattern of the Sohm Abyssal Plain sediments surrounding the Congress and Lynch seamounts; this facies abuts directly against topographically opaque hills (profiles M–N, O–P) or the acoustically transparent pattern (profiles G–H, I–J), or both; the layered facies is commonly disrupted by a reflection-free, diapir-like pattern of unknown origin (for other explanations see legend for Figure 5).

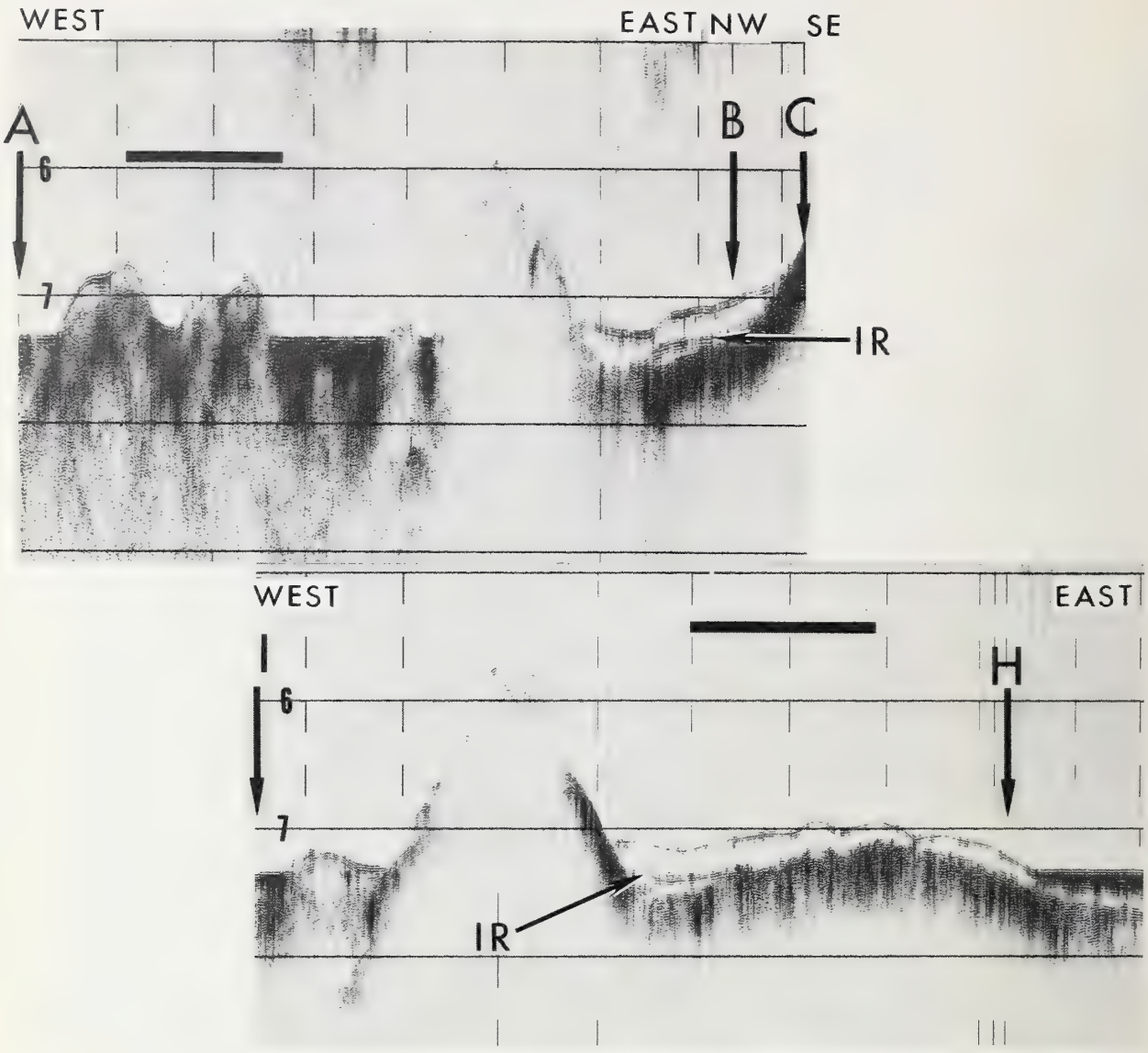

FIGURE 9.—Seismic profiles showing acoustically transparent sediment north of the northern Congress peak; the internal reflectors (IR) are areally more limited than in the perched basin, compare with profiles in Figure 7 (for other explanations see legend for Figure 5).

This layered series directly abuts the base of the seamounts, in sectors where the acoustically transparent layer is absent (Figure 7, profile J–K, and Figure 5, profile E–F).

The Sohm Abyssal Plain almost always displays the acoustically layered facies overlying acoustically transparent or opaque seismic reflection patterns; we presume the latter to be basement. Sediment thicknesses range from about 0.15 to 0.5 seconds (one-way travel time) between areas of relief on the basis of *Vema* (Figure 4) and *Lynch* profiles. The contact between the layered and the opaque basal seamount flank facies is well illustrated in the 3.5 kHz records obtained while underway to and from CTD Station 2 on the southern Congress peak (Figure 10, profile *c*).

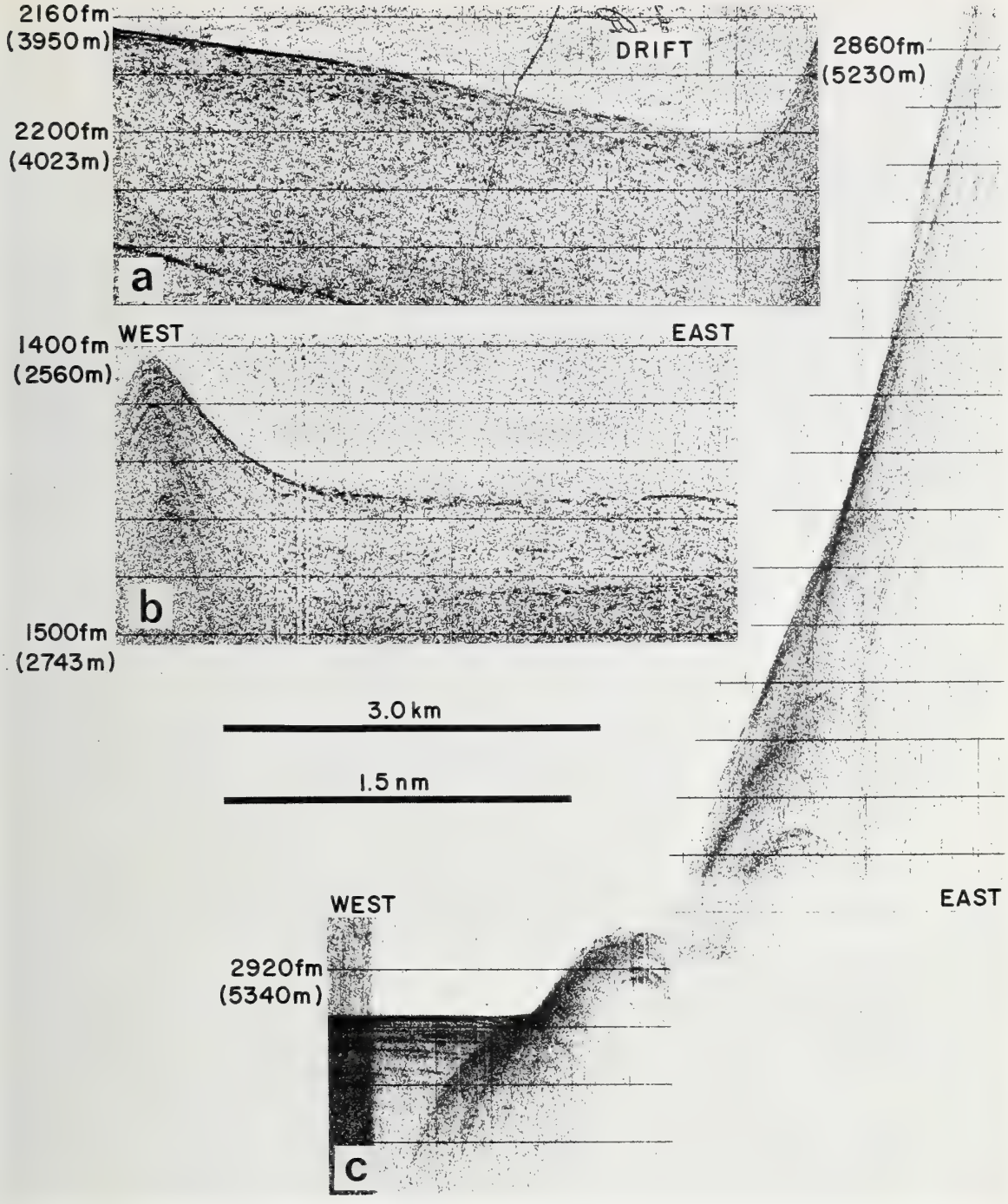

FIGURE 10.—Selected 3.5 kHz subbottom profiles obtained near (*a*, *b*) and west (*c*) of the southern Congress peak (location of profiles shown in Figure 2); compare the subdued layering of sediment in profiles *a* and *b* with the distinctly layered Sohm Abyssal Plain sediments abutting the base of the mount *c* (horizontal scale applies to profiles *b* and *c*; profile *a* made while ship was drifting).

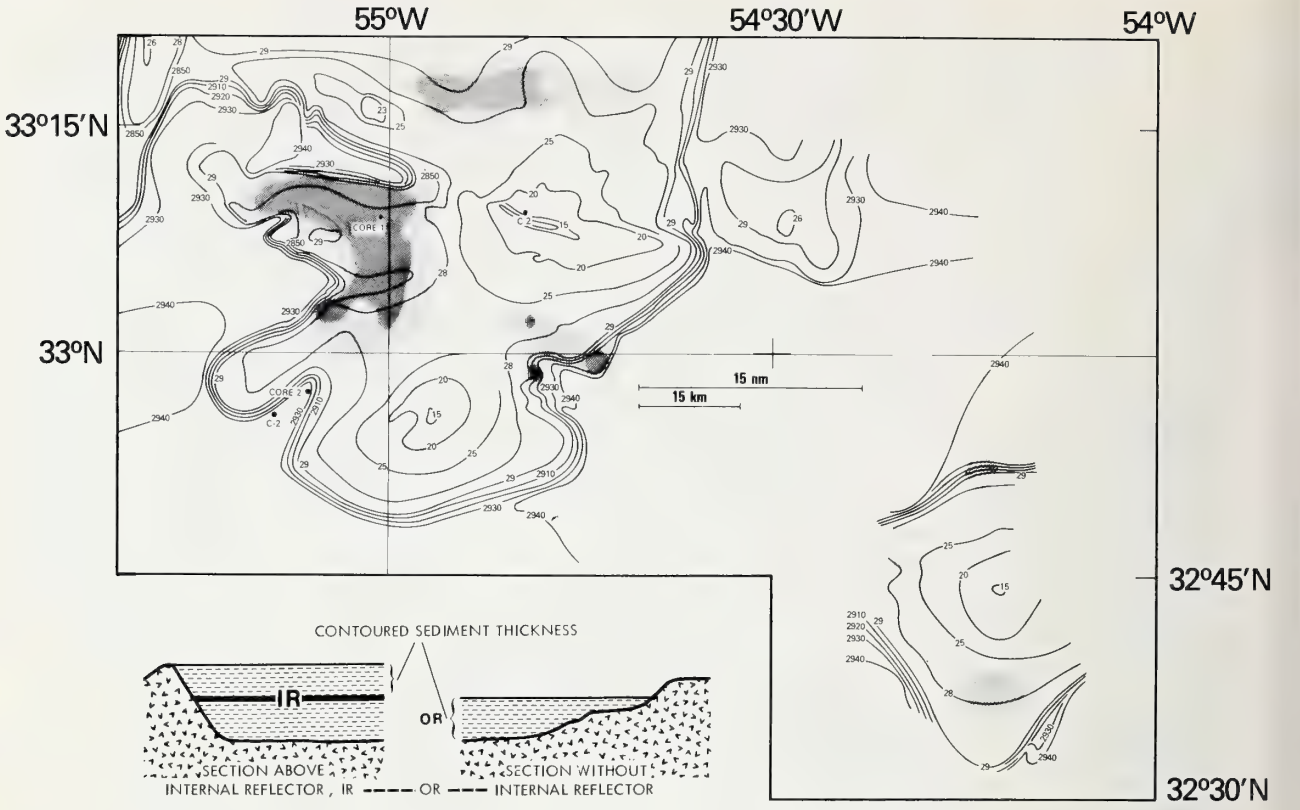

FIGURE 11.—Isopach map of acoustically transparent facies, showing two sedimentary configurations: sections above internal reflectors (IR) and sections without an internal reflecting horizon (dense stippling pattern = sediment thicknesses >0.20 seconds of two-way travel time; lighter stippling = 0–0.20 seconds).

PERCHED SEDIMENT BASIN.—The largest areal distribution and thickest section of unconsolidated sediment above the acoustic basement of the Congress Seamount is situated to the west of its northern peak (Figures 11, 12). At this location, sediment has accumulated in a saddle between the two major peaks in a depression bounded to the west by a nearly continuous topographic ridge (Figure 7, profiles J–K and N–O). Sediment in this perched basin comprises both distinct and weak acoustically layered material as illustrated by Figures 7 (profile J–K) and 13. Maximum thickness of this material ranges to about 520 m, assuming a velocity of 1.90 km/sec (cf. Houtz, 1974). Three distinct and continuous reflectors forming the top 75 m thick section in *Lynch* profiles are an acoustic artifact, i.e., multiple reflections from the sediment-water interface caused by several bubble pulses produced by the seismic sparker. The high-resolution 3.5 kHz records along the same traverse show marked lateral variation rather than continuity of the upper sediment layers (Figure 10).

Within this large sediment basin, another series of distinct multiple reflectors (hereafter referred to as internal reflectors, IR) occur at about 200 m below the sediment-water interface (Figure 7, arrow on profile J–K; Figure 13). This IR, unlike the reflecting horizon at the sediment-water interface, is probably composed of several horizons of distinct acoustic impedence, and it divides this thick sequence of weakly layered facies (Figure

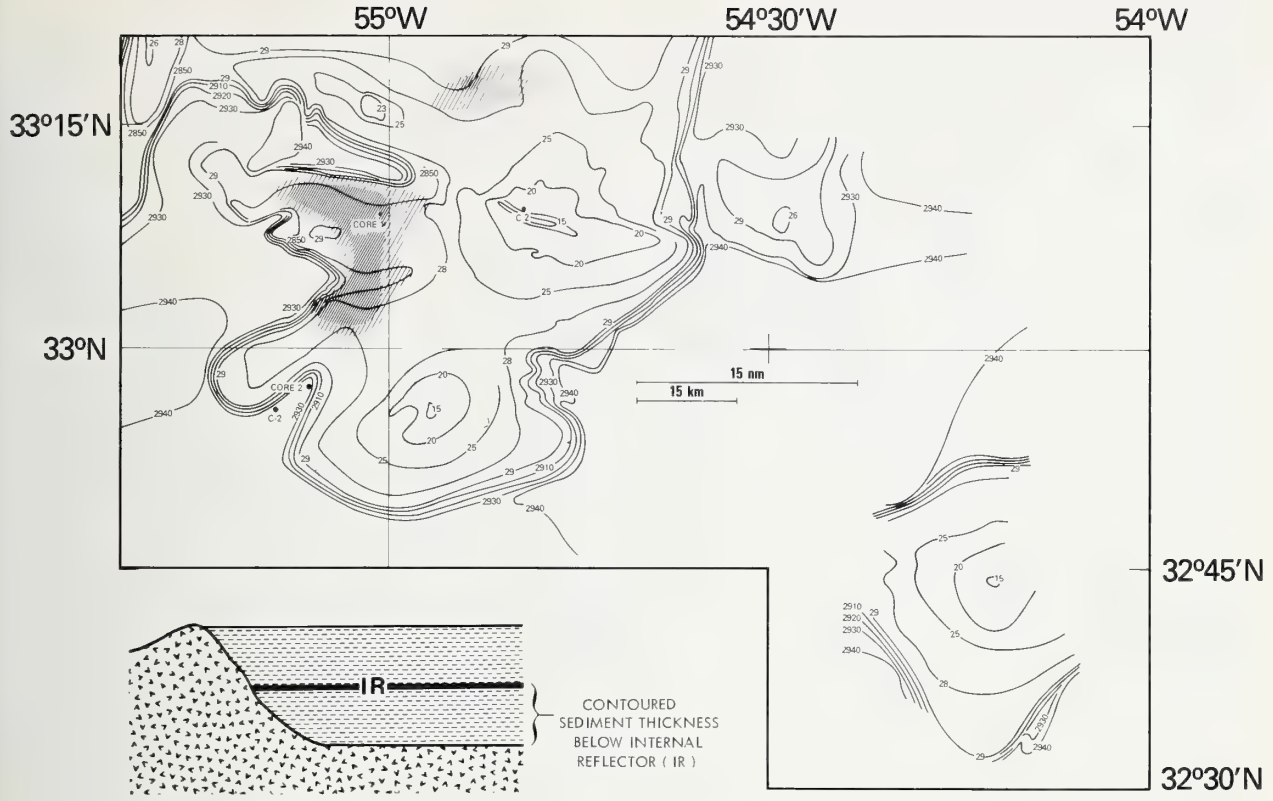

FIGURE 12.—Isopach map of acoustically transparent facies beneath internal reflectors (IR); note that IR presence is restricted to regions north and west of Congress peak (dense hatching = thicknesses beneath IR >0.20 seconds of two-way travel time; light hatching = 0.10 to 0.20 seconds).

13). At the thickest point 285 m of sediments lie above (Figure 11), and 235 m lie below (Figure 12), this IR.

OTHER AREAS NEAR CONGRESS AND LYNCH SEAMOUNTS.—A depositional configuration comparable to the perched basin cited above (two layers of acoustically transparent sediment separated by strong IR) also occurs in the sector north of the northern peak of Congress (Figures 3, 9, 11, and 12). Elsewhere in the region surveyed, including the Lynch Seamount, smaller ponds of acoustically transparent sediment occur without the IR (Figures 6 and 11).

The thick (380 m) accumulation of acoustically transparent material situated to the north of Congress thickens westwardly, and abuts the base of another large ridge (Figure 9, profile H–I). A short north-south seismic traverse west of the northern peak (Figure 8, profile I–J) shows thickening of the acoustically transparent facies in a southerly direction; the southern termination of this facies is abruptly truncated by the acoustically layered facies of the Sohm Plain. The greatest thickness of transparent series (about 140 m) on the Lynch Seamount lies northwest of the peak (Figures 6, 11), while thinner accumulations are found north and south of the peak. High-resolution 3.5 kHz profiles also show the indistinct, more poorly defined layering that characterizes the thin accumulation of acoustically transparent facies on the upper Congress flank (Figure 10, profiles *a* and *b*).

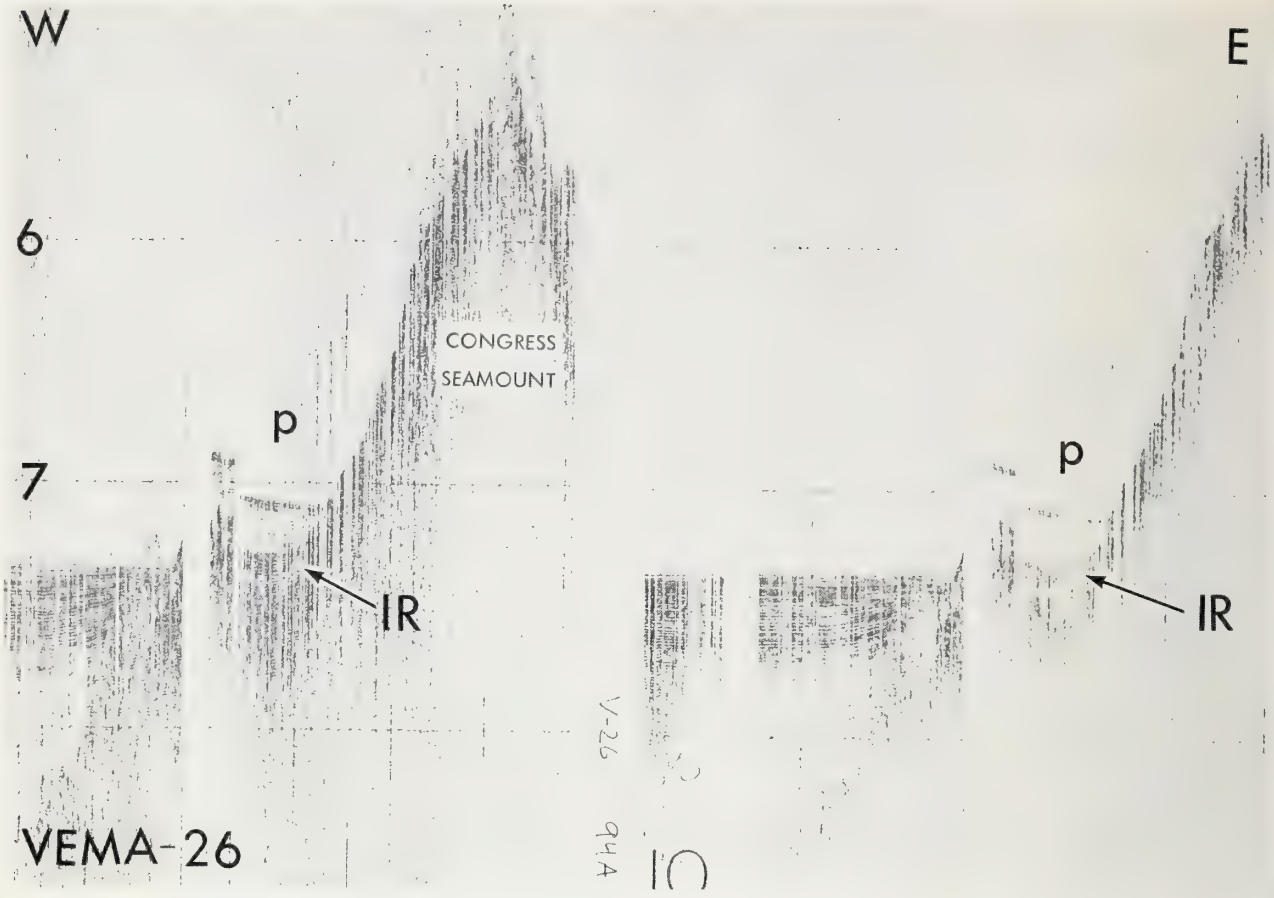

FIGURE 13.—*Vema* 26 airgun profiles of one sector of seafloor west of the Congress Seamount (for location see Figure 3, also cf. 4A), showing perched basin (p) and internal reflectors (IR); left profile is a high-pass filtered record that reveals layering in the "acoustically transparent" section above IR; right profile is a low-pass filtered record, in which layering above the internal reflectors IR, is absent; note that the reflector at the sediment-water interface at p is layered in both sections suggesting that this is an acoustic artifact (both profiles were made on 8 August 1968 between 1100 and 1300 hours; reproduced from Ewing et al., 1974, with permission from the Lamont-Doherty Geological Observatory).

Core Lithologies: General Description

In this and the following sections we describe the petrologic characteristics of five cores in the following sequence (Figure 1): southern Sohm Abyssal Plain proper (*Atlantis* 153-141, *Vema* 22-231, and *Lynch* 710-78-2); on, and adjacent to, the surrounding flanking hills (*Vema* 26-6 and 26-9); and perched basin on the lower flank of the Congress Seamount (*Lynch* 710-78-1).

The *Atlantis* core is by far the coarsest of the five and includes numerous, distinct, coarse sand layers, particularly in the lower two-thirds of the section (Ericson et al., 1961, fig. 11). Contacts between the layers of sand, muddy sand, and mud are generally sharp, as revealed by distinct changes in grain size and color. Sand layers, some in excess of 10 cm, may consist of largely biogenic components (commonly foraminifera), or mixed biogenic and terrigenous fractions. In the lower part of the core, however, terrigenous material predominates. The sand layers, some graded, are

probably turbidites. Colors, recorded only after the core had dried, are yellowish brown and olive grey.

Vema core 22-231, while only 30 km to the west and lying about 185 m deeper than the *Atlantis* core, displays a significantly different lithology. It is composed almost exclusively of silty clay and clayey silt, with only rare thin silt and sand layers. Coarse sand layers are generally graded and micaceous and are interpreted to be turbidites. Some finer-grained sections display bioturbation, while others comprise varve-like silt laminations that occur irregularly and could represent fine-grained turbidites. The effect of bottom-current activity, however, cannot be discounted. From the Lamont core log description, the section consists of alternating moderate- to reddish-brown (5YR4/4), pale-brown (10YR6/2), and light-olive-grey (5YR5/2) units. Some darkly streaked zones apparent in split cores consist of iron sulfide-rich layers often related to burrowing structures.

In contrast to the *Vema* 22 core, *Vema* 26-6 and 26-9 are fine textured, more homogeneous, and do not display distinct sand or silt laminae. They do, however, show localized patches of light, almost cream-colored sections 1 to 5 cm thick. These patches have been interpreted as weathered volcanic products, possibly palagonite (unpublished L-DGO core descriptions, 1969). Both cores recovered largely foraminiferal silty clay that includes only a minor fraction (1 percent or less) of terrigenous or nonforaminiferal biogenic components. The cores display moderate-yellowish-brown (10YR5/4), moderate-brown (5YR3/4) and light-brown (5YR6/4) sections. Some units show intensely burrowed structures.

Core *Lynch* 710-78-1, from the perched basin, most closely resembles *Vema* core 22-231 in terms of vertically varying grain size (clayey silt and silty clay) and a cyclic pattern of sedimentation (Figure 14). The down-core variation in the *Lynch* core is characterized by fine-grained ooze (30% pelagic organisms) of different colors: pale-brown (10YR6/2) mud, alternating with yellowish-brown (10YR4/2) and moderate- to reddish-brown (5YR4/4) mud layers. Most of these layers range from about 20 to 50 cm thick, although two of them exceed 1 m. Textural analyses (Table 1) show that the yellowish-brown (and in some cases grey) layers are clayey-silt ooze dominated by silt, with minor proportions of sand. The moderate- to reddish-brown ooze layers tend to be thinner and somewhat finer grained (silty clay) than the yellowish-brown muds (as shown in Figure 14). Two features of this core are a distinct angular truncation at about 435 cm, and highly bioturbated zones with large vertical and/or horizontal (transverse) burrows located at about 210, 330, 500 and 540 cm (sections at 210, 330, and 500 cm are noted on x-radiographs, Figure 15). A distinct vertically graded sand (largely foraminifera) to mud layer in the pale-brown zone is clearly observed between 303 and 290 cm; an x-radiograph (Figure 15) shows that this unit actually fines upward to about 275 cm. It is interpreted as a turbidite.

Rates of Sediment Accumulation

Five radiocarbon dates were obtained on samples collected from core *Lynch* 710-78-1 (Figure 14). Results, listed below, are in years before present, and centimeters refer to sample depth below core top: 11,070±85 at 12–20 cm; 11,160±500 at 20–30 cm; 22,390±470 at 170–185 cm; 33,760±800 at 260–274 cm, and >43,000 at 310–325 cm. Rates of accumulation in centimeters per 1000 years or cm/ka, between these dated horizons are approximately <2, 13, 13.5, 8, and <4.5; a time integration of the overall sedimentation rate is approximately 7 cm/ka. It is noteworthy that the highest rates apply to the yellowish-brown mud immediately below the significantly more slowly accumulating Holocene core top (Figure 14). This yellowish-brown layer accumulated between 40 and 165 cm from approximately 20,000 to 12,000 B.P., about the time of the most recent eustatic low sea level stand, followed by a rapid sea level rise. This was a cold period during and following major glaciation at the end of the Pleistocene (Laine, 1978). We also obtained two dates from *Vema* 22-231, on the plain proper, nearest the *Lynch* core: 31,700±1400

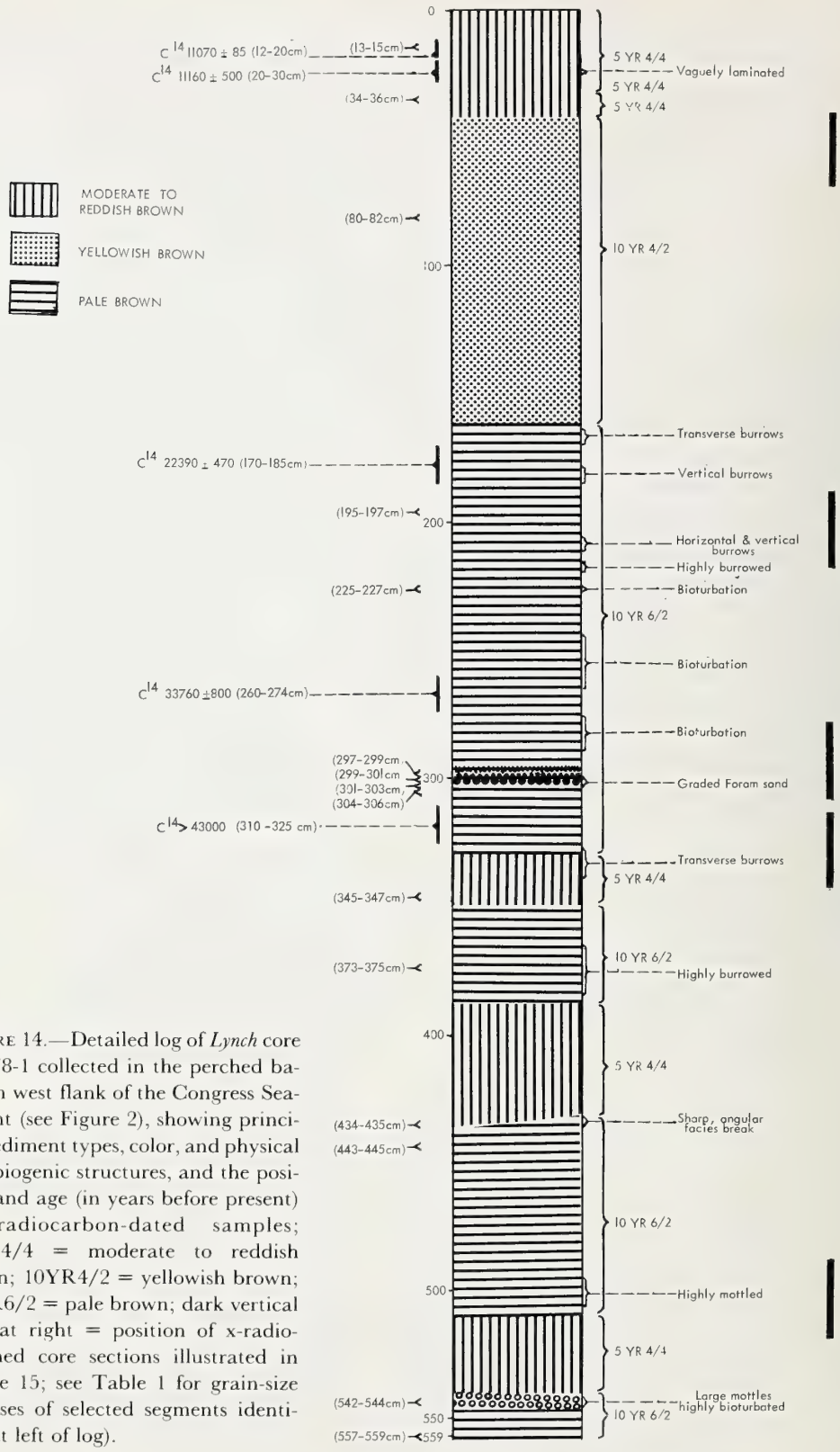

FIGURE 14.—Detailed log of *Lynch* core 710-78-1 collected in the perched basin on west flank of the Congress Seamount (see Figure 2), showing principal sediment types, color, and physical and biogenic structures, and the position and age (in years before present) of radiocarbon-dated samples; (5YR4/4 = moderate to reddish brown; 10YR4/2 = yellowish brown; 10YR6/2 = pale brown; dark vertical bars at right = position of x-radiographed core sections illustrated in Figure 15; see Table 1 for grain-size analyses of selected segments identified at left of log).

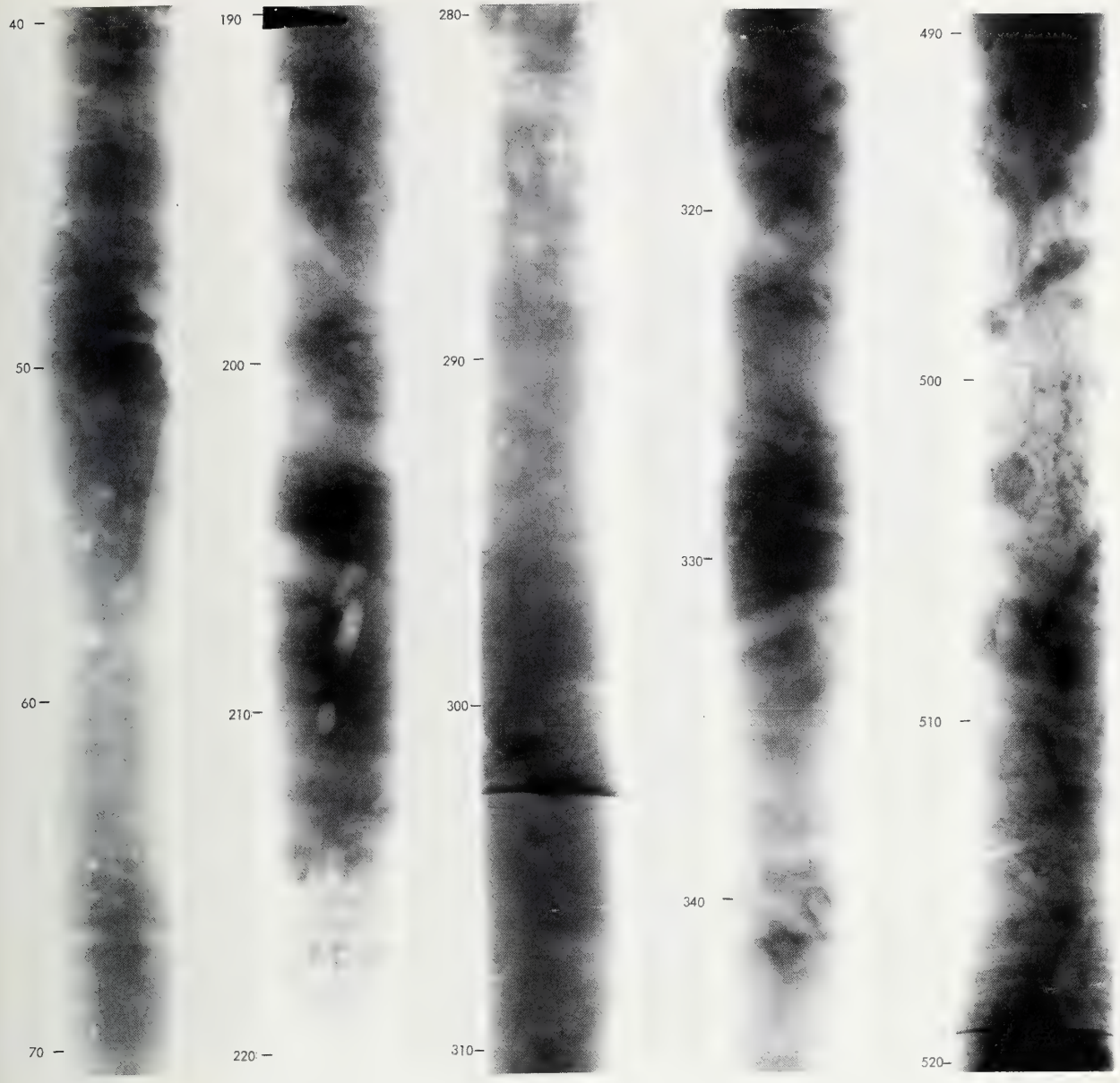

FIGURE 15.—X-radiographic prints of selected sections of *Lynch* core 710-78-1 collected in the perched basin on the west flank of the Congress Seamount (position of sections in centimeters below core top as shown in core log in Figure 14), revealing various degrees of bioturbation including some horizontal and vertical burrows, and completely reworked mottled sections, and a graded turbidite consisting of bioclastic sand to clayey silt (303 cm to 280 cm).

at 44–45 cm, and 37,500±1500 at 89–100 cm. Rates of accumulation between these dated horizons are about 1.5 and 7.5, and the averaged rate is about 2.5 cm/ka, lower by a factor of three than the *Lynch* perched basin section. In both cores, the presence of sharp contacts between layers indicate probable hiatuses. The tops of these two cores may not have been recovered and, therefore, computed rates should be used with caution.

In order to compare our values with the rates of sedimentation for areas bounding the Sohm Plain we examined data from two Deep Sea Drilling Project and one Giant Piston Core sites. These data reveal extreme areal variability in the accumulation of sediment. The rates in the southern Sohm Plain are comparable to averaged long-term accumulation values (about 12 cm/ka) for the Quaternary and Upper Pliocene sections forming the abyssal plain at the base of the Nashville Seamount (JOIDES drill site 382) about 150 km northwest of the Congress (Tucholke and Vogt, 1979). In contrast, extreme variations occur in the hills bordering the southern sector of the plain. On the lower flank of the Mid-Atlantic Ridge to the east, near *Vema* 26-6, JOIDES drill site 10 revealed a considerably reduced Quaternary section. Very low sedimentation (<1 cm/ka) perhaps affected by sediment compaction, is recorded there (Peterson, Edgar, et al., 1970). To the west of the plain, however, radiocarbon dates from a Giant Piston Core (GPC site 5) reveal rates two orders of magnitude higher than were measured near the Congress Seamount (Silva et al., 1976). In brief, these highly variable rates can be explained in large part by regional removal and subsequent redeposition of sediment resulting from large-scale water-mass circulation (see earlier sections on sediment acoustic facies distribution and Figures 4 to 12).

Textural and Compositional Characteristics

Grain Size.—Size analysis included the sand (>63 μm), silt, and clay (<2 μm) fractions. These results are presented in Table 1, and graphically depicted by bars in Tables 2 to 5.

The upper third of *Atlantis* core 153-141 consists of low proportions of sand; samples below 400 cm, however, contain abundant (locally to >65%) sand. The silt/clay ratio in the upper third of the core is highly variable, recording alternating amounts of silty clay and clayey silt. Below 400 cm the core is generally characterized by greater proportions of silt than clay (Table 2).

In contrast, *Vema* core 22-231 is largely mud (silt and clay mixtures, Table 1) and contains a few, thin sand layers (Table 3). The silt/clay ratio is usually greater than 0.5, and the core includes larger proportions of silty clay than does the *Atlantis* core. *Vema* cores 26-6 and 26-9 are even finer grained than the above, and contain only traces of sand and a range of low to very low (0.57–0.14) silt/clay ratios (Table 4). This analysis highlights the prevailing silty clay texture and generally homogeneous nature of these two abyssal hill cores.

Lynch core 710-78-1 recovered in the perched basin on the Congress Seamount flank is most similar to, but somewhat siltier than, Sohm Plain *Vema* core 22-231 (Table 5). One distinct turbidite (sand to clayey silt) occurs at about 300 cm (Figures 14, 15). Overall, this core is characterized by highly variable silt/clay ratios ranging from about 0.5 to 2.7 (Table 1).

Coarse Fraction Composition.—Size analyses show that, with the exception of *Atlantis* core 153-141, most samples contain a low proportion (<1% or trace) of sand. A semiquantitative estimate of the proportion of the 16 most common components of the coarse fraction (>15 μm)—coarse silt and sand—of selected samples is depicted in Tables 2 to 5.

The coarse fraction of the upper part of core *Atlantis* 153-141 is dominated by sand of biogenic origin (largely planktonic foraminifera) and carbonate fragments, with smaller amounts of other bioclastic, terrigenous, and apparently volcanic components (Table 2). In the lower two-thirds of the core, quartz, heavy minerals, and mica of sand size prevail. Volcanic products (optically

identified palagonite, sideromelane, and chlorophaeite) are found locally, and occur as present-to-few throughout (Table 2).

The coarse-fraction composition of *Vema* 22-231 is much more variable than for the *Atlantis* core: some samples are dominated by biogenic components, others by terrigenous, and some include both (Table 3). Moreover, the proportion of volcanic products is also highly variable, with the highest concentration near the core top (probably due to winnowing). The biogenic fraction is largely carbonate fragments (predominantly broken foraminifera) and coccoliths rather than unbroken foraminiferal tests. Manganese micronodules, siliceous aggregates (probable volcanic alteration products), and plant fibers are irregularly distributed in this core (Table 3).

Cores *Vema* 26-6 and 26-9 are distinct from the above cores primarily by their uniformly high proportion of volcanic and related products, including manganese micronodules (L. A. Barnard, pers. comm.; see also Figures 16, 17), siliceous aggregates (Figure 16), devitrified glass, palagonite, zeolites and altered feldspars (Figure 17), and pyroxenes. This assemblage argues against a dominantly diagenetic origin. Moreover, evidence for reworking is provided by the presence of quartz along with high proportions of carbonate fragments and coccoliths in the upper parts of the cores (Table 4).

Core *Lynch* 710-78-1 is most similar to core *Vema* 22-231 in that the coarse component assemblages vary vertically, and are dominated by carbonate fragments (broken foraminifera), whole foraminiferal tests, and coccoliths; siliceous aggregates and brown mica are also present, with smaller proportions of weathered glass, spicules, radiolaria, quartz, and other light and heavy minerals (Table 5). The difference between Sohm Plain core *Vema* 22-231 and *Lynch* core 710-78-1, which was obtained at more than 325 m above the plain on the flank of Congress, is that the latter contains substantially lower amounts of quartz, no plant matter and a somewhat higher proportion of volcanic products (Table 5), including manganese micronodules. Petrographic microscope and Scanning Electron Microscope (SEM) analyses of the *Lynch* coarse silt fraction show variable proportions of mica, plagioclase feldspars, siliceous microfossils (Figure 18A,B), calcareous nannofossils (Figure 18C,D), foraminiferal fragments (Figure 18C,D), dolomite rhombs (Figure 18E), and angular volcanic shards (Figure 18F). Palagonite, sideromelane and/or chlorophaeite are found in every sample examined throughout the core. The abundance of these volcanic products, usually of coarse silt-size, varies considerably from sample-to-sample (Table 5).

Many of the carbonate microfossils in the *Lynch* core are poorly preserved (Figure 18), possibly from dissolution and recrystallization. The moderate- to reddish-brown layers contain a much higher proportion of siliceous microfossils and a lower proportion of coccoliths than the yellowish-brown layers (Figure 18A). In many samples of the latter sediment facies, as well as in the graded bed (at 300 cm), mixed faunas comprising Late Quaternary (Figure 19A), Tertiary (Figure 19B,C), and Upper Cretaceous (Figure 19D) are found (C. C. Smith, pers. comm., 1980). The benthic foraminifera in the graded bed at about 300 cm provide evidence of downslope displacement of at least 1000 m; their original habitat is normally about 3000 to 4000 m (S. Streeter, in litt., 1979). Other layers in the cores also indicate displacement of benthic foraminifera.

Further insight on modification of faunal content related to dissolution associated with depth is provided by *Lynch* core 710-78-2, essentially a surficial Sohm Abyssal Plain seafloor sample. This small core is a clayey silt with a trace of sand (>63 μm) that consists largely of foraminifera and mica grains; it is texturally and mineralogically analogous to the upper samples of *Lynch* core 710-78-1. The foraminifera, however, tend to be somewhat more poorly preserved than in *Lynch* core 1; thin tests that break easily during preparation may have been affected by deposition below the carbonate compensation depth (CCD).

Fine Silt and Clay Fraction Composition.—X-ray diffraction analyses of the less than 2 μm size fraction from all cores examined confirm the

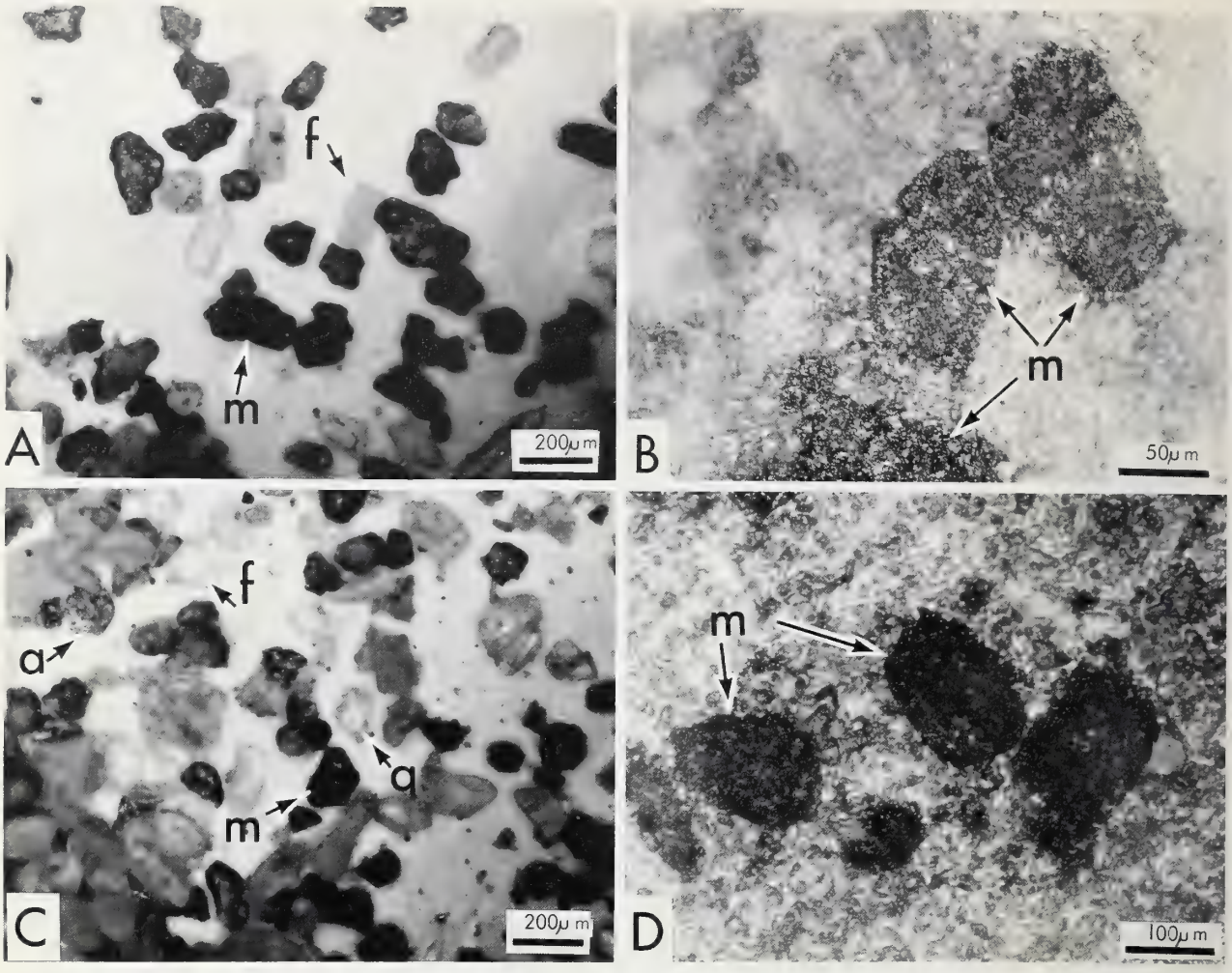

FIGURE 16.—Photomicrographs of selected samples from core *Vema* 26-9: A and C, sand fraction from 435–437 cm and 503–505 cm, respectively, showing manganese micronodules (m), feldspars (f), quartz (q) and siliceous aggregates (a); B and D, sectioned micronodules from 453–457 cm and 503–505 cm, respectively, mounted in Lakeside© cement (matrix) and viewed in reflected light; the manganese-rich grains show no obvious internal structure (scale in μm).

patterns of clay-mineral distribution found in this general region by Biscaye (1965).

Core *Atlantis* 153-141 (Table 2) illustrates that the clay-mineral suite throughout is dominated by the mica group (illite, muscovite). Kaolinite and chlorite together account for about a third of this size fraction, while feldspars and calcite account for the remainder. Montmorillonite (used in this paper synonymously with smectite) occurs only in trace amounts.

The silt-fraction suite is dominated by plagioclase, dolomite, and calcite. In addition, mica, kaolinite and chlorite, quartz, K-feldspar, and amphibole are generally present in variable proportions.

The clay-size fraction from core *Vema* 22-231 (Table 3) is generally comparable to the *Atlantis* core. The composition of silt is also similar, but shows a slightly higher amount of dolomite.

The clay-mineral fraction of cores *Vema* 26-6 and 26-9 (Table 4) is markedly different from the previously discussed cores in that the proportion

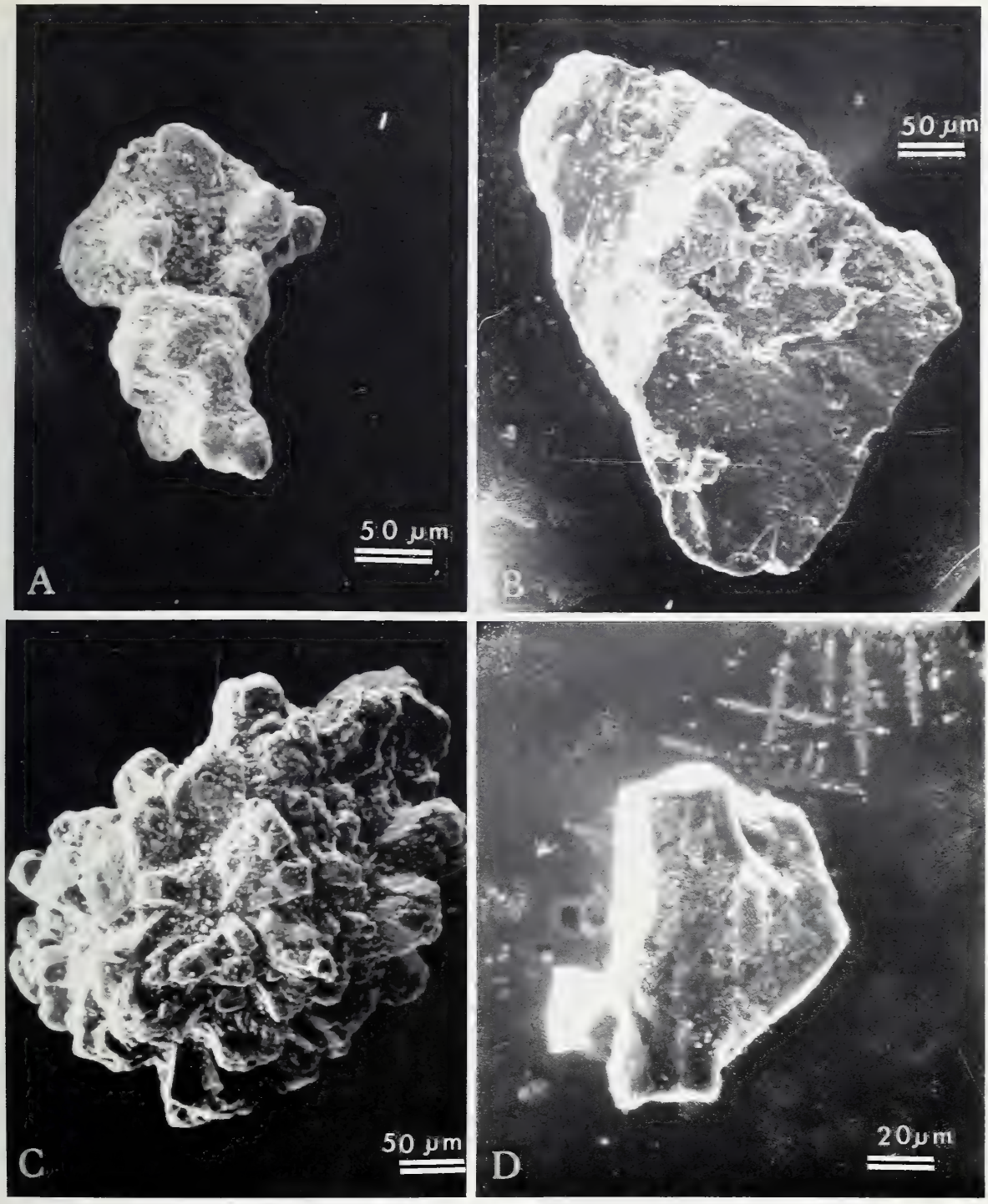

FIGURE 17.—Scanning electron micrographs of selected grains from *Vema* 26 cores: A, manganese micronodule (*Vema* 26-6, 474–476 cm); B, palagonite glass (*Vema* 26-9, 503–505 cm); *c*, zeolite (phillipsite, note twinning) in *Vema* 26-6, 474–476 cm; D, plagioclase feldspar, weathered and iron-coated (*Vema* 26-6, 45–47 cm) (scale in µm).

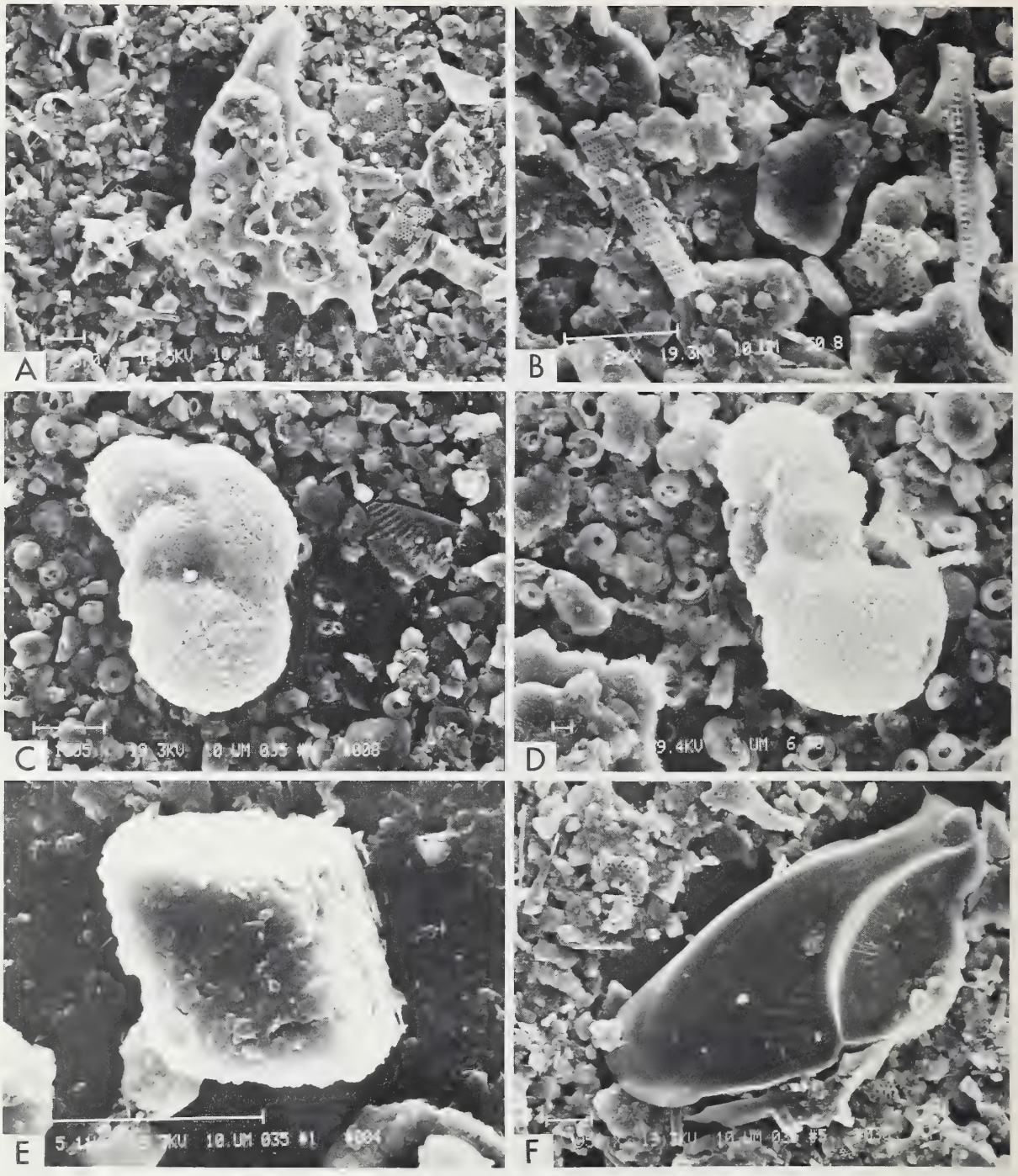

FIGURE 18.—Scanning electron micrographs of selected samples from *Lynch* core 710-78-1: A, B, dominantly siliceous fraction (silicoflagellates and diatom fragments) from the moderate to reddish-brown and pale brown facies, 345 and 374 cm, respectively, from the top of the core; C, D, carbonate fraction dominated by coccoliths and recrystallized foraminifera from the yellowish brown facies, 14 and 302 cm, respectively; E, dolomite rhomb, 14 cm; F, volcanic shard, 226 cm (scale given by thin horizontal bar in μm).

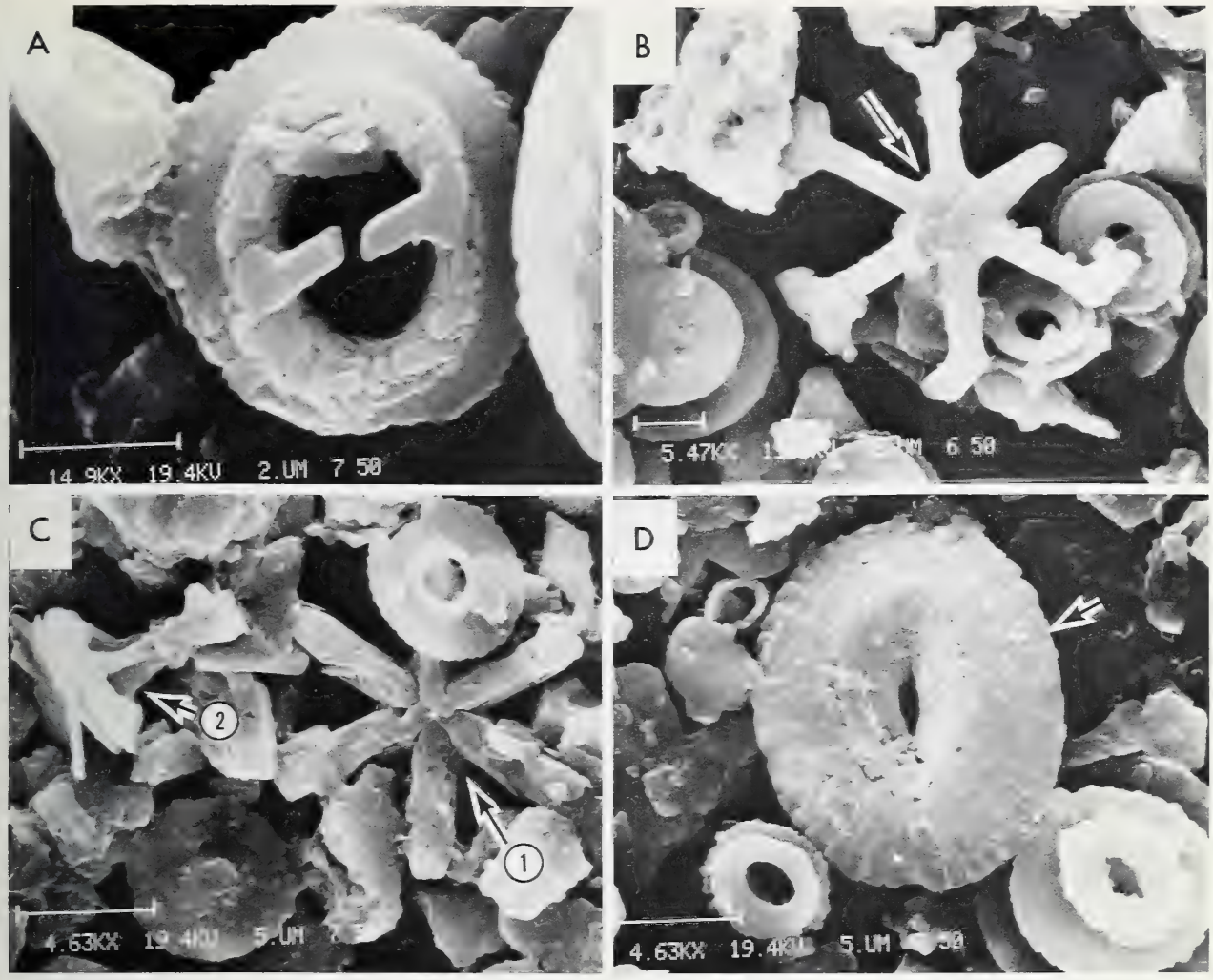

FIGURE 19.—Scanning electron micrographs of selected microfossils in *Lynch* core 710-78-1: A, *Gephyrocapsa oceanica*, a typical Quaternary coccolith species (at 543 cm from the top of the core) commonly found throughout this core and mixed with the reworked species illustrated in the other components of this illustration; B, *Discoaster variabilis* (arrow) of Middle Miocene to Pliocene age (at 301 cm); C, *Discoaster* (arrow 1) of probable Pliocene age and *Prediscosphaera cretacea* of Cretaceous age (arrow 2) at 543 cm; D, *Watznaueria barnesae* (arrow) of Cretaceous age at 543 cm (scale in μm).

of montmorillonite is generally over 25%, and ranges up to about 50%. Moreover, the relative percentages of kaolinite plus chlorite are somewhat higher than those of the mica group. With regard to the silt fraction, these two *Vema* cores generally contain higher mica, kaolinite plus chlorite, and plagioclase, with notably lower calcite than the *Atlantis* and *Vema* 22 cores.

The *Lynch* core 710-78-1 (Table 5) clay-size samples contain montmorillonite in amounts greater than in *Atlantis* or *Vema* 22-231 cores, but lower than the two *Vema* 26 cores. The mica group, moreover, is more abundant than the kaolinite and chlorite components, and the proportion of quartz is about the same as in the *Vema* 26 cores. In the silt fraction of the *Lynch* core, the

dolomite is usually present, calcite amounts are extremely variable, and the proportions of mica, kaolinite, and chlorite are more similar to the *Vema* 26 cores. Amphibole is not detected, but samples from the four other cores yield traces to 5%. X-ray diffraction mineralogy reveals a generally lower calcite content in the silt- and clay-size fractions, and X-ray fluorescence shows a substantially higher iron and, in some instances, manganese content in the moderate- to reddish-brown layers of the *Lynch* core.

X-ray fluorescence analyses of manganese and iron in the clay-size fractions from the five cores reveal rather consistent concentrations of iron throughout these samples. The relative amount of manganese, however, is extremely variable (values expressed as counts per 0.1 mg per 200 seconds; see Tables 2–5): in the *Atlantis* core, values range from 3.2–7.8; *Vema* 22, 6.2–10; *Vema* 26-9, 8.3–32.5; *Vema* 26-6, 7.1–60.9; and *Lynch*-1, from 1890 to 4620. We interpret the thousand-fold increase from the *Atlantis* to the *Lynch* core to be a result of the latter's proximity to the volcanic Congress Seamount. In contrast, the lowest values in the *Atlantis* core result from its greater distance to volcanic sources and dilution by terrigenous and biogenic components. It may be noted that energy dispersive x-ray analysis of a typical micronodule (Figure 16) of the sand-size fraction from the *Lynch*-1 core (Table 5) highlights the values of the two most abundant elements: manganese, 27,555, and iron, 13,365 (lesser amounts of copper, nickel, zinc, chromium, and cobalt also are measured). These results are comparable to electron microprobe analyses from *Vema* 26 cores that indicate some micronodules of coarse silt and fine sand size (Figure 17A) are comprised largely of manganese, iron, and nickel. We note that these manganese micronodules are associated with palagonitized glass (Figure 17B), zeolites (probably phillipsite, Figure 17C), smectites (montmorillonite, Table 4), and plagioclase feldspar (Figure 17D). This assemblage occurring in *Vema* 26 cores 6 and 9 is generally diagnostic of altered volcanic materials (cf. Peacock and Fuller, 1928; Arrhenius, 1963; Honnorez, 1978; Stonecipher, 1978; Scott et al., 1979). Some of these products, such as smectite, may also have been derived from land sources.

Water-Mass Movement

The general circulation in the Atlantic, summarized by Wüst (1949; and Heezen and Hollister, 1971), shows the dominance of the Arctic and Antarctic water masses on abyssal circulation. A recent hypothesis concerning the circulation in the Northwest Atlantic proposed by Worthington (1976, fig. 11) shows a major NNE–SSW elongated gyre related to the Gulf Stream system. This large clockwise-rotating gyre is located east of Cape Hatteras, extends to about 40° W longitude, and is positioned over the Bermuda Rise and most of the Sohm Abyssal Plain. It is believed to influence the circulation pattern of the deeper waters, including those above the southern Sohm Abyssal Plain (Schmitz, 1977; Laine, 1978).

Two CTD vertical profiles through the water column were made on the western flanks of the Congress Seamount to ascertain the nature of the intermediate and deep waters in the study area. CTD Station 1 was situated on the perched basin about 3 km east of core *Lynch* 710-78-1, and CTD Station 2 was obtained on the southern peak (Figure 2). Three distinct water masses are recognized: North Atlantic Central Water, extending from the surface to a depth of about 930 m (510 fm); a second layer, about 170 m thick, composed in part of Mediterranean Water, ranging from 930 m (510 fm) to about 1100 m (600 fm); and below this, North Atlantic Deep Water, extending almost to the bottom of the profiles on the flanks of the seamount. The presence of Antarctic Bottom Water (−0.5°C, 34.65‰) is suggested by the lowermost readings of the temperature-salinity curve. The profiles indicate the possibility of slight mixing of Antarctic Bottom Water with North Atlantic Deep Water at, and just above, the sediment-water interface on the lower flanks of the seamount and on the abyssal plain (D. Greenewalt, in litt., 1979). While these data are admittedly limited, they tend to support the

oceanographic model of Wüst (1949), Heezen and Hollister (1971, fig. 9.45), and others that show the northward extension of the Antarctic Bottom Water to the region encompassing the southernmost part of the Sohm Abyssal Plain.

Since current-meter data are lacking, an indication of water flow and direction is obtained by noting the nature of bedforms recorded by compass-oriented bottom photographs. Three camera stations located around the Congress Seamount (Figure 2), reveal predominant transport from SSE to NNW. This flow direction at the three localities was determined from ripple marks (Figures 20, 21), craig-and-tail features (Figure 22), coarse lag accumulated against obstacles on the bottom (Figure 20A), and asymmetrically deformed mud structures (Figure 22). Although this bottom transport pattern may probably represent only recent and short-term dispersal, it is noteworthy that (a) the isopach map indicates localized thickening of sediment south, north, and west of both Lynch and the northern peak of Congress (Figure 11), and (b) selected seismic profiles show accumulation of transparent acoustic series east of obstacles (Figure 9, profile H–I). These latter observations could be interpreted as the result of long-term sediment dispersal trends toward the north and west quadrants. These patterns tend to support the oceanographic model of a westerly-directed return flow of the southern leg of the Gulf Stream Gyre above the Sohm Plain study area (Worthington, 1976; Laine, 1978).

Discussion and Conclusions

A review of sedimentation models in the abyssal plains of the Atlantic and other world oceans reveals an emphasis on gravitative processes, largely turbiditic, and long distance dispersal of terrigenous material, primarily sands (e.g., Heezen and Laughton, 1963). There is, in fact, ample documentation for the Northwest Atlantic Basin that the processes of turbidity currents and related gravity flows of sediment account for a significant proportion of abyssal plain deposits, especially the sands (Horn et al., 1971; Pilkey et al., 1980). In addition to this particular land-derived component, most workers also call attention to the contribution from clastic particulate matter, of both terrigenous (fine silt and clay) and biogenic (largely planktonic tests) origin, which settle from suspension. The deposits from these two differing modes of sedimentation have been interpreted from seismic profiler data and core analyses. Sediments lacking internal acoustic reflectors ("acoustically transparent" layers) are generally inferred to be pelagic or resuspended deposits which may be composed of well-bedded clays (Fox et al., 1967), foraminiferal ooze with clays (Taylor and Hekinian, 1971), or a complex mixture of clay, sand, and carbonate-rich layers (Silva et al., 1976). The relative proportion of carbonate tests within these pelagic sediments, largely foraminifera and coccoliths, tends to be highest in areas shallower than the carbonate compensation depth (CCD). In contrast, distinct acoustic reflectors revealed by seismic profiler data and coarse silt- to sand-sized sediment recovered in cores are generally thought to have formed as turbidites.

Recent studies show that clay- to sand-size sediments emplaced by either turbidity currents or pelagic suspensate deposition can be, and probably in most instances are, modified by the action of bottom currents (Heezen and Hollister, 1971; Laine, 1978). Evidence for this bottom-current erosion in the southern Sohm Abyssal Plain study area includes lineated bedform features revealed by photographs (Figure 22), textural properties of the coarser-grained fractions (Hubert, 1964), and the age measurement (in excess of 30,000 yrs B.P.) near the top of core *Vema* 22-231, which reveals a truncated upper sediment layer.

All of the above depositional mechanisms emphasize distal transport. We note in abyssal plain studies, however, that the role of proximal or more local-intrabasinal sediment source and dispersal (in particular, the displacement of volcanically derived sediments, cf. Heath and Dymond, 1977) is for the most part neglected. This is indeed surprising if one views a physiographic chart of

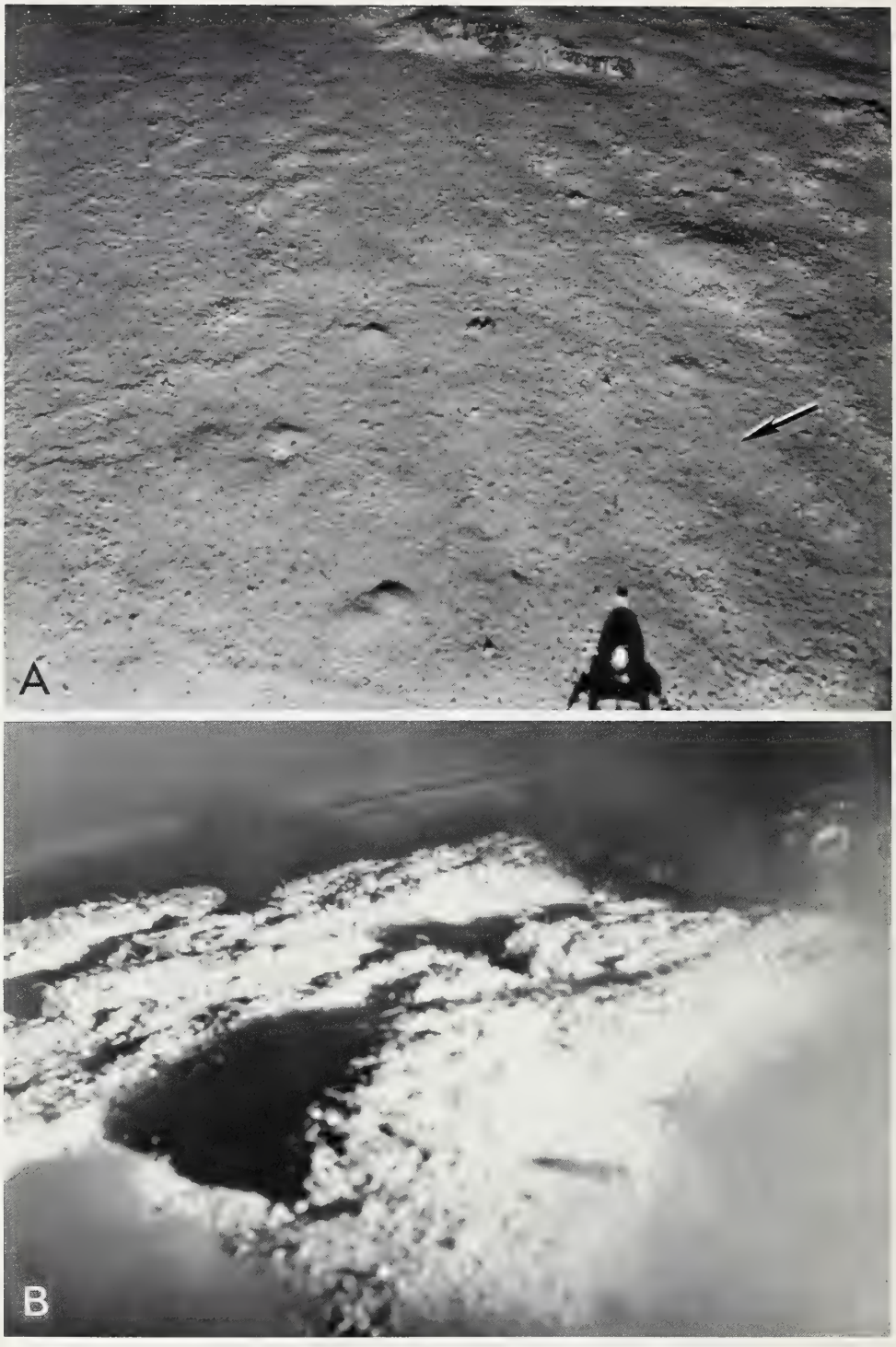

FIGURE 20.—*Lynch* 710-78 camera station 1, oblique view bottom photographs on the northern Congress peak (between 3110–3290 m, location shown in Figure 2): A, subdued asymmetric ripples of sand and mud transported toward NNW (arrow), note coarse lag against small outcrop in background; B, mixed biogenetic-volcanigenic sediment veneer of bedrock, presumably volcanic, note distinctly rippled sediment in background (compass diameter = 6.3 cm).

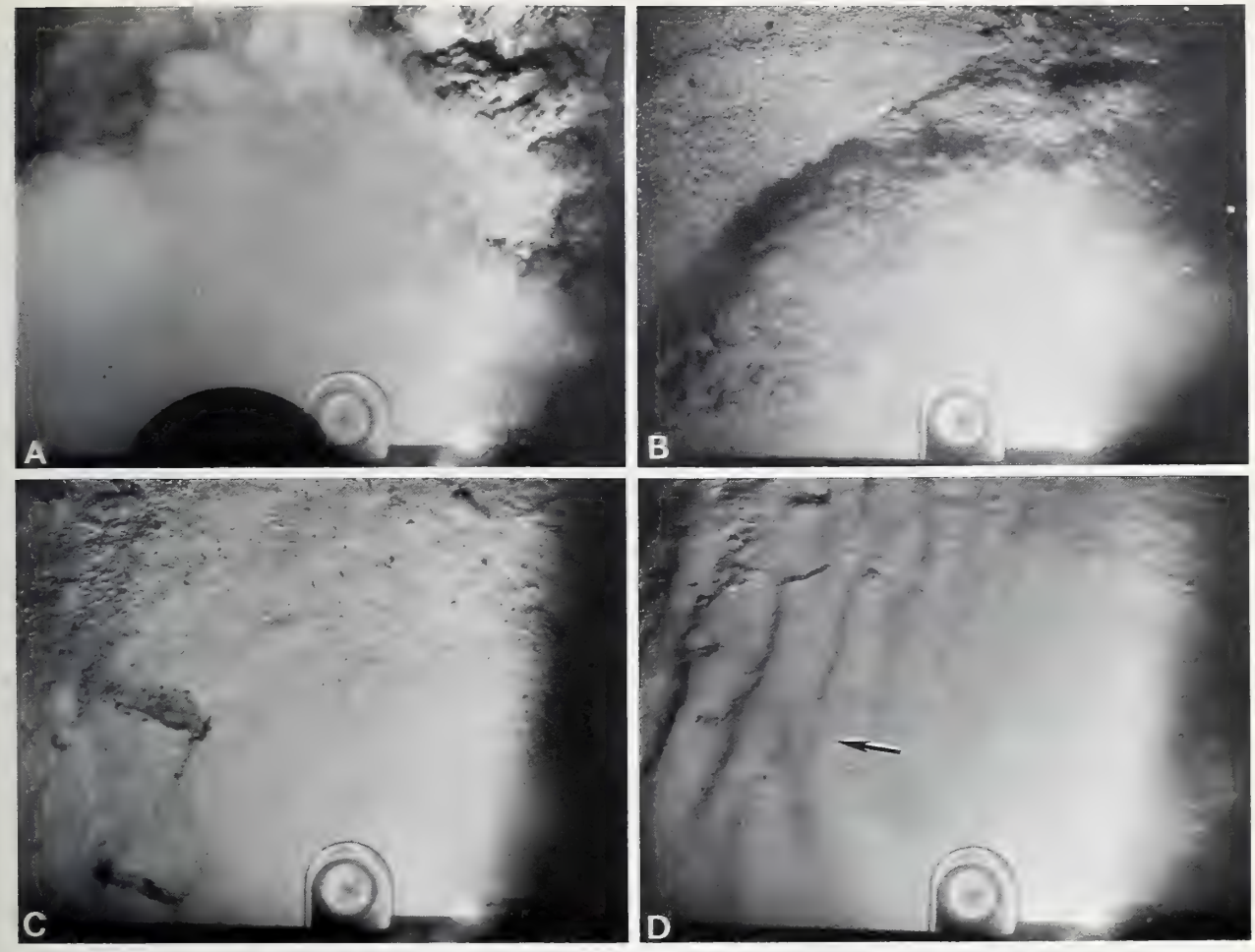

FIGURE 21.—*Vema* 26 camera station 7 vertical-view bottom photographs on the southern Congress peak (between 2815 and 2850 m, location shown in Figure 2): A, B, volcanic pillows thinly covered by sediment mantle; C, very coarse biogenic-volcanigenic sediment and rock fragments; D, asymmetric ripples of muddy sand transported almost due north (arrow) (compass diameter = 7 cm; photos courtesy of Lamont-Doherty Geological Observatory of Columbia University).

the oceans (Heezen and Tharp, 1968), which reveals a ubiquitous, highly variable vista dominated by positive topographic relief (ridges, fracture zones, abyssal hills, seamounts, knolls, etc., many shown on Figure 1) of predominantly volcanic origin.

It is pertinent with respect to the problem of proximal versus distal provenance that our study area is situated in the southermost section of the Sohm Abyssal Plain because (a) it has received a dominant proportion of its sediment fill by turbidity-current processes, with materials derived largely from the Canadian Maritime Provinces (Horn et al., 1971); (b) it underlies the region of densest suspended particulate matter, or nepheloid layer, concentration (>3000 $\mu g/cm^2$) in the North Atlantic Ocean (Biscaye and Eittreim, 1977, fig. 5); (c) it is influenced by bottom-current activity (bottom photographs and seismic data, this study) resulting from large scale bottom-water circulation (Worthington, 1976; Laine, 1978); and (d) it lies near the geographic center of the

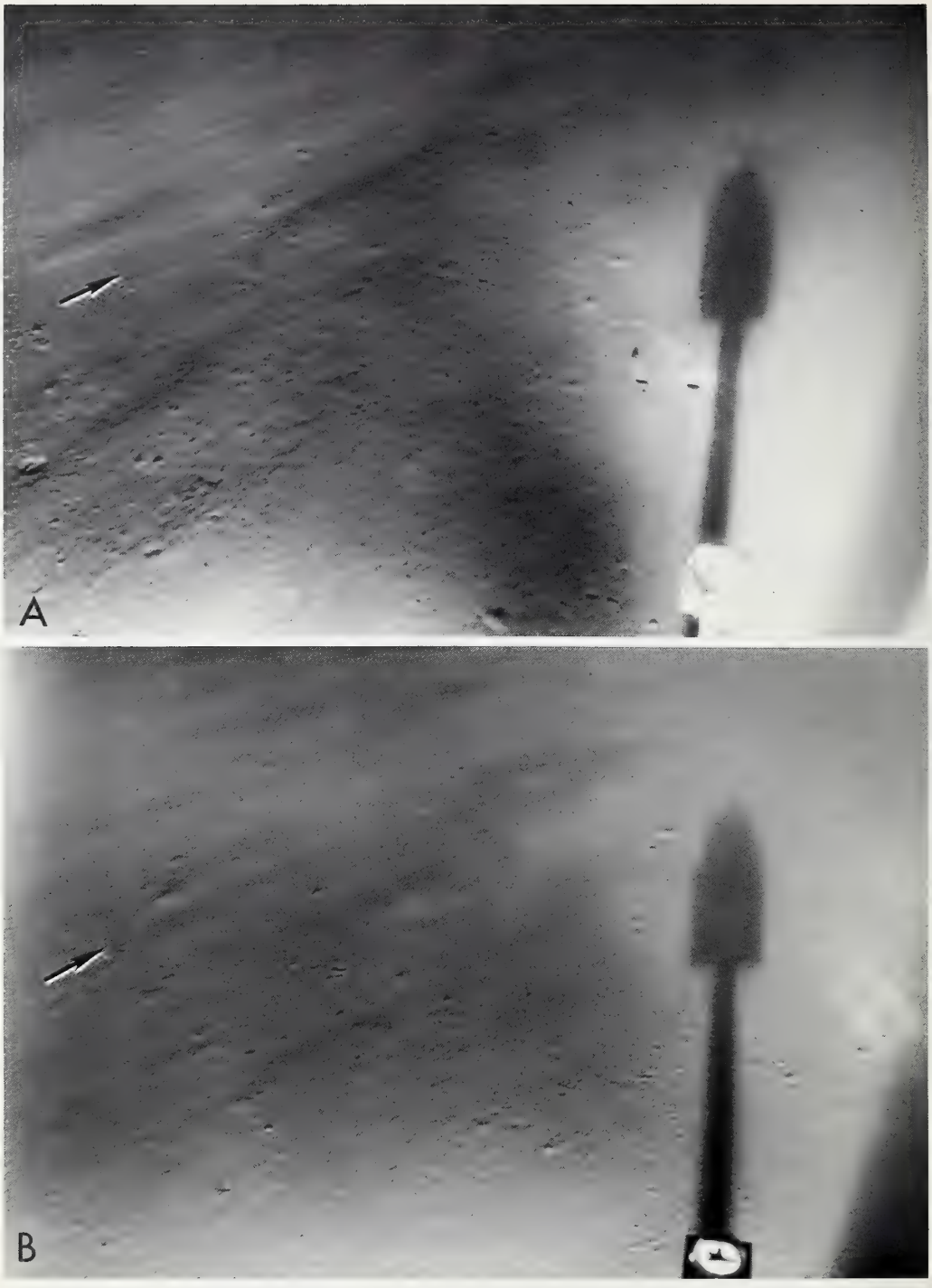

FIGURE 22.—*Lynch* 710-78 camera station 2, oblique-view bottom photographs on Sohm Abyssal Plain west of the southern Congress peak (about 5365 m, location shown in Figure 2): A and B reveal small craig-and-tail features and asymmetrically deformed mud structures oriented toward the northwest (arrows) (compass diameter = 6.3 cm).

Northwest Atlantic Basin, remote from land sources and almost completely surrounded by major volcanic features (including the lower flanking hills of the Mid-Atlantic Ridge, Bermuda Rise, and Kelvin and Corner Rise seamounts, see Figure 1 and also Ewing et al., 1973). Thus, the Southern Sohm Abyssal Plain is an appropriate area to evaluate the role of more proximal and volcanically derived sediments.

On a global scale, abyssal plain sediments consist of variable mixes of the following: (a) land and continental margin-derived clastics (including ice-rafted debris) and/or bioclastic materials; (b) suspensates of clastic (including wind-blown) and biogenic origin; (c) authigenic sediment and diagenetic products; and (d) volcanically derived materials. As in the case of most abyssal plains that have direct access to both land and continental margin-derived materials, the southern Sohm Plain piston cores reveal a dominant terrigenous fraction. This is best illustrated by core *Atlantis* 153-141. As in many other cores from this large abyssal plain, the significant proportion of terrigenous material was initially emplaced by turbidity current flows (Horn et al., 1971; Pilkey et al., 1980). All four Sohm Plain cores we examined also show an important pelagic component (e.g., core *Vema* 22-231) that is related to the well-defined distribution pattern of the suspension-rich, benthic nepheloid layer (Biscaye and Eittreim, 1977). Nevertheless, we have found that all cores have at least some silt- and even sand-size volcanic components (Tables 2–5). Despite the significant amounts of land-derived turbidite sediments that dominate abyssal plain cores *Atlantis* 153 and *Vema* 22, significant amounts of volcanic materials, including palagonite and manganese micronodules, are present (Tables 2, 3).

The proportion of these volcanically derived products is related to the proximity of the cores to volcanic physiographic features of varying relief; see, for example, the large concentration of volcanic products near the top of core *Vema* 22-231 (Table 3) and the position of this core relative to volcanic physiographic highs (Figure 4B). Our study clearly demonstrates that cores *Vema* 26-6 and -9, from an area near the margins of the Sohm Plain bounded by abyssal hills and shielded from clastic land sources, contain a considerably enhanced fraction of volcanically related material of clay as well as silt and sand sizes (Table 4). These components include manganese micronodules, zeolites, palagonite, chlorophaeite, sideromelane, and smectite. Some of these materials are almost certainly supplied from the submarine weathering of basalt and its alteration products (Arrhenius, 1963; Nayudu, 1971; Honnorez, 1978; Scott et al., 1979; Furnes, 1980). We do not exclude the possibility that some of these components were derived from diagenetic remobilization (i.e., manganese micronodules, see Scott et al., 1979) and/or from distal land sources (smectite).

As a test of the true importance of this allochthonous volcanically derived component in the Sohm Abyssal Plain setting, we examined core *Lynch* 710-78-1, which was recovered from a sediment basin perched about 400 m above the abyssal plain on the flank of Congress Seamount (Figures 2, 7). About 500 m of sediment has accumulated in this elevated and isolated basin. The principal significance of the *Lynch* core location is that it is shielded from the direct influence of large-scale, bottom-hugging turbidity currents, which tend to follow along deeper contours of the abyssal plain.

From the *Lynch* seismic survey, it is apparent that distribution of the ponded sediment series is largely controlled by local topography and bottom-water flow. In this respect, the perched basin serves as a particularly valuable example (Figures 11, 12). Most of the ponded sequence in this basin, while acoustically transparent to the sparker seismic frequency (about 100 Hz), is in effect layered (Figure 13) when insonified with airgun frequencies (about 20 Hz). Sections of core *Lynch* 710-78-1, from this pond, particularly the moderate- to reddish-brown layers (see horizons labeled 5YR4/4, Figure 14), provide evidence of pelagic deposition. The upper reddish-brown layer, deposited in post-Pleistocene time, and sim-

ilar deeper horizons (Figure 14) are characterized by the following: (1) clay mineral assemblages of the type occurring throughout this North Atlantic region (Biscaye, 1965) but also including an enhanced fraction of montmorillonite; (2) an abundance of planktonic microfossils including foraminifera (often poorly preserved and recrystallized), radiolaria, and other siliceous microfossils whose proportions vary markedly vertically; (3) a very fine-grained texture (largely silty clay); (4) accumulation rates that for the most part are less than 3 cm/ka; (5) vague laminations and intensely bioturbated layers (Figure 15); and (6) the presence of siliceous agregates (Table 5) that may have been produced by benthic activity accompanying slow deposition, or may be of biogenic opaline derivation (T. C. Huang, pers. comm., 1980).

To help explain the above, we recall that the study area lies within the region of highest suspended particulate matter concentration in the North Atlantic Ocean (Biscaye and Eittreim, 1977). Moreover, Congress Seamount is located adjacent to a zone of marked bottom-current activity related to the westward-directed return flow of the southern Gulf Stream Gyre (cf. Worthington, 1976). Three bottom photograph stations (Figures 20–22) provide evidence for seafloor erosion, inferring flowing water on and around the seamount. Thus, the pelagic deposition in the perched basin is complicated by the interaction with moving bottom water in this region.

In addition to this pelagic transport regime, the marked cyclic nature of core *Lynch* 710-78-1 (Figure 14) shows that other modes also were responsible for deposition in this pond during the Quaternary. In comparison to the reddish-brown layers, the thicker, but somewhat less oxidized, yellowish-brown ooze layers (Figure 14, see horizons labeled 10YR4/2) have (a) somewhat larger proportions of better preserved planktonic foraminifera and calcareous nannofossils, and (b) tests of the latter, many of which are obviously reworked from older strata and dated from Pliocene to Upper Cretaceous (Figure 19); also, they (c) are coarser grained (clayey silt); (d) may display graded bedding (Figure 15, 303–280 cm); and (e) record much higher rates of accumulation (locally 13 cm/ka) in the Upper Pleistocene. Such layers probably account for some subdued, discontinuous reflectors noted on 3.5 kHz profiles (Figure 10). Emplacement of this sediment type, particularly the graded beds, is almost certainly by gravitative mechanisms, including turbidity currents.

The ubiquitous, but irregular, abundance in this *Lynch* core of coarse silt- to sand-sized volcanic products, including primary (sideromelane, angular glass shards) components and secondary alteration derivatives (palagonite, chlorophaeite, zeolites), plus the importance of montmorillonite in the clay fraction indicate a steady, important supply of weathered material to the pond from an igneous source (Table 5). These products are associated, in some instances, with reworked microfossils as old as Upper Cretaceous (Figure 19). The proximity of the sediment pond to the seamount and other adjacent basement rises suggests that these igneous features are major-source terrains. In addition to this igneous supply, material reworked from the older depositional cover draping these basement rises also appears to serve as a sediment source (cf. Taylor and Hekinian, 1971). This volcanic-biogenic assemblage is similar to that described by Van Andel and Komar (1969), Nayudu (1971), and others. Bottom photographs show that currents on these bathymetric highs are capable of eroding and transporting weathered volcanic material along with microfossil-rich (pre-Quaternary to Recent) pelagic sediments and the recently deposited suspensates (Figure 20). This combined regime of suspensate deposition and reworking by bottom-current activity has resulted in accumulation of mixed biogenic-volcanigenic deposits on the seamount. These materials subsequently fail on the relatively steep slopes of the mount and adjacent highs and are resedimented to greater depths by a complex mechanism involving bottom current, creep and mass flow, including turbidity-current (cf. Stanley and Taylor, 1977). Specific examples of downslope displacement are provided by the graded

foraminiferal sand bed (Figure 14, base at 303 cm) and by the displacement of benthic foraminifera to a depth of at least 1000 m below their normal range as recorded in various layers of the *Lynch* core.

The perched sediment fill in the basin thus reveals a complex history of depositional processes: suspensates plus older locally derived pelagic deposits subsequently have been reworked by bottom currents and displaced downslope by gravitative mechanisms. Sediments derived from more distal sources supplement these ponded deposits in the perched basin. These latter distal materials would likely include resuspended Sohm Abyssal Plain sediments transported by bottom currents (Biscaye and Eittreim, 1977; Laine, 1978). Wind-blown silt, some of which may include a volcanic dust (cf. Huang et al., 1975, 1979; Sigurdsson et al., 1980), may also be a minor distal component. In addition, the measured accelerated rate of sedimentation in the *Lynch* core during the period from about 20,000 to 12,000 years B.P. (Figure 14) almost certainly records large-scale oceanographic phenomena that affected extensive parts of the North Atlantic during the late Pleistocene. These factors influencing the transport of material from distal sources to the southern Sohm Plain include eustatic oscillations coupled with important changes in the composition and circulation pattern of deep-water masses associated with the advances and retreats of polar fronts (Schnitker, 1974, 1979; CLIMAP project members, 1976; Ruddiman, 1977; Ruddiman and McIntyre, 1976, 1979; Duplessy et al., 1980; and others).

The perched sediment basin well illustrates a situation where there has been a concentration of an important contribution of volcanic-rich material emplaced by bottom-current erosion of the adjacent seamount and by coarse-grained mud flows, turbidity currents, and related submarine gravity flows. During a period of unknown duration, these mass flows resulted in the deposition of distinct volcaniclastic (possibly hyaloclastite) layers characterized by a distinct acoustic contrast, the internal reflectors (IR), within the sediment series (Figure 13). The areally restricted distribution of the internal reflectors in the depressions west and north of the northern Congress peak (Figure 12) also indicates a local derivation and a probable volcanic origin. While no direct evidence for the origin or nature of these reflectors is available, similar seismic reflection profiles showing large acoustic impedences have been drilled west of the study area (Tucholke and Vogt, 1979; Bowles, 1980). This drilling revealed volcaniclastic layers.

The IR acoustically "hard" layer can be traced almost uniformly across the perched basin (Figure 7, profile J–K); elsewhere around the Congress Seamount, the more restricted distribution of the internal reflectors is observed (Figure 9, profile A–B–C). The well-defined IR horizon is a small-scale example of an acoustic reflector comparable to the one covering a large area in the Northwest Atlantic Basin surrounding Bermuda, Horizon A^v (Tucholke and Mountain, 1979; Bowles, 1980). The Worzel ash layer (Worzel, 1959) in the eastern Pacific, while having a subaerial explosive volcanic origin, also produces a similar seismic profiler record.

In general, the transport processes and resulting deposits that have accumulated in the Congress Seamount perched basin appear analogous to locally derived sediments revealed in and around other igneous regions, such as rises, ridges, seamounts, and rifts as illustrated by Heezen and Hollister (1971, their chapters 12 and 13). In particular, depressions in physiographically complex terrains tend to trap and concentrate locally derived sediments, including material from volcanic terrains and products of submarine weathering (Honnorez, 1978). An example includes the Nazca plate of the eastern Pacific (Heath and Dymond, 1977). In the northwest Atlantic, near the study area, are occurrences of volcanic-rich and mixed volcaniclastic and biogenic oozes concentrated in depressions within fracture zones and minor bathymetric lows on the Mid-Atlantic Ridge (Fox and Heezen, 1965; Siever and Kastner, 1967; Van Andel and Komar, 1969; Latouche and Parra, 1979; Scott et al., 1979).

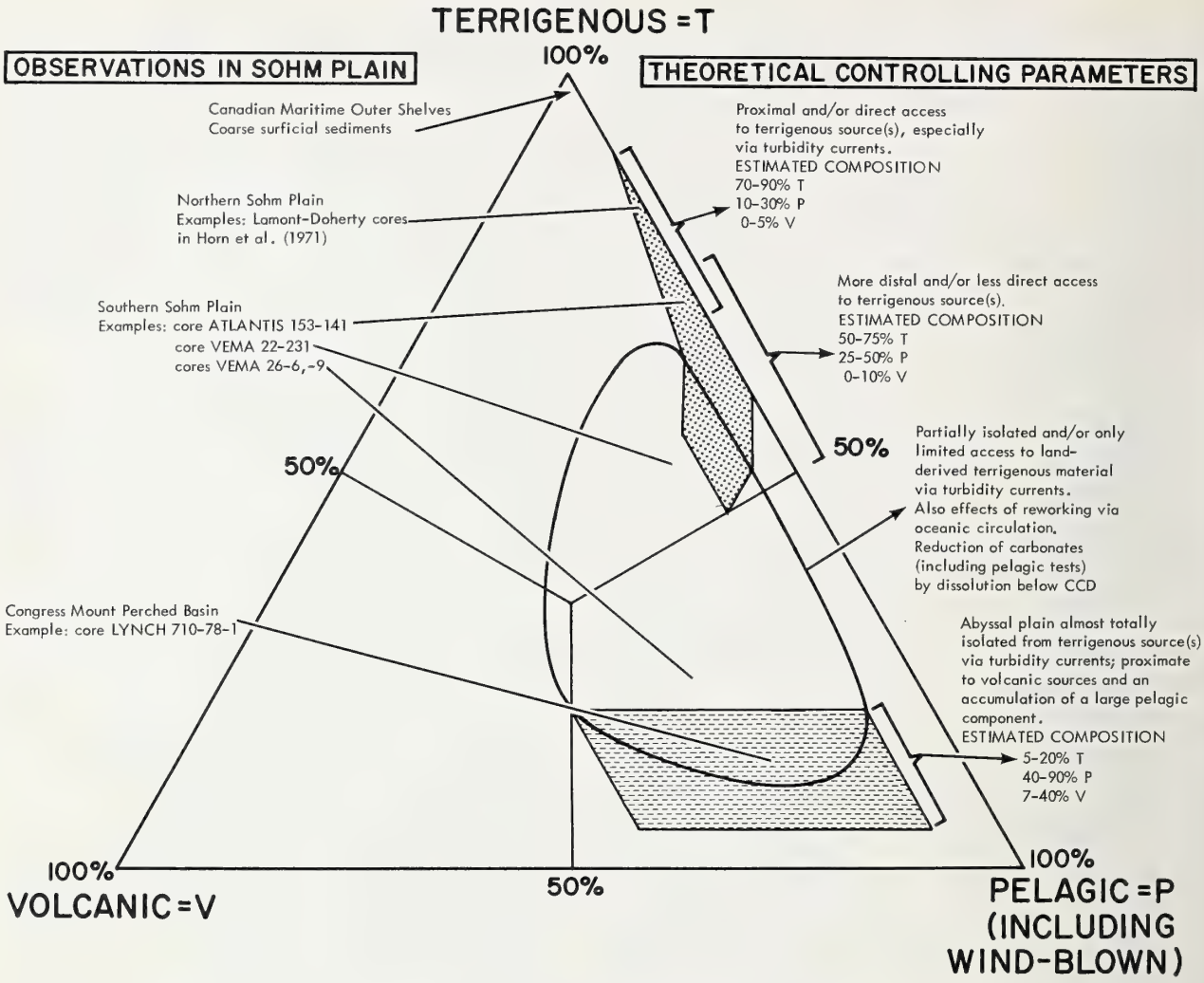

FIGURE 23.—Deposition model depicting different origins of sediment in the southern Sohm Abyssal Plain based on volumetric compositional analyses from this study. This scheme involves three major components: terrigenous (including bioclastic), pelagic (including wind-blown), and volcanic. This model indicates processes and is suggested to apply for abyssal plains in general.

Where topographic damming is absent on the eastern and southern flanks of Congress Seamount (Figure 12), such locally derived volcanic and reworked mixed volcaniclastic-biogenic materials are disseminated on the surrounding Sohm Abyssal Plain. In these instances, sediment provided from nearby volcanic topography is present, but in minor amounts, i.e., dispersed and masked within the reworked terrigeneous turbidite and biogenic suspensate sequences of the Sohm Plain as illustrated by the *Atlantis* and *Vema* 22 cores (Tables 2, 3).

On the basis of the above, it is reasonable to expect that where the terrigenous supply is either blocked by positive or negative bathymetric features or markedly diminished (perhaps by distance from source), the proportion of pelagics and/or volcanics would be enhanced. To illustrate how volcanics can be used as an index or "yardstick" of modes of abyssal plain sedimenta-

tion, a simple diagram is presented (Figure 23). This scheme uses a ternary diagram as a framework in order to illustrate the temporal or spatial sediment distribution. The three end-members of this triangle represent the major components of sedimentation: terrigenous, pelagic (including wind-blown), and volcanic materials (and their alteration products). Two distinct fields are recognized: one is dominated by terrigenous or terrigenous plus pelagic components; the other comprises largely pelagic or pelagic plus volcanic components. The former field (dot pattern on Figure 23) illustrates the masking of the pelagic and volcanic fraction by the preponderance of land-derived clastics in areas adjacent to land sources or along turbidity current paths. Thus, as distance increases or as access to land-derived sources diminishes, the proportion of the terrigenous component is decreased. In contrast, abyssal plain sediment accumulating in a region almost totally isolated from terrigenous sources would include primarily the pelagic and volcanic components (i.e., the latter field, dashed pattern in Figure 23).

This simplified pattern in the Sohm Abyssal Plain is complicated by dynamic factors such as fluctuations of large-scale bottom-water circulation and the variability of the depth at which the dissolution of carbonate (CCD) occurs (e.g., Jansa et al., 1979; Thiede et al., 1980; and others). These factors would explain downcore variability in carbonate test content and the significant areal variation in sediment rates observed in, and adjacent to, this study area. These physical oceanographic conditions result in the blurring of the distinction between the two major fields as depicted by the closed curve in Figure 23. There are obviously many possible ways in which these factors would apply. For example, moving bottom waters can winnow and/or transport locally derived volcanics (cf. Huang, 1980) and older weathered sediments to areas remote from their provenance. In another case, increased rates of carbonate dissolution (due to changes in the CCD) could reduce the numbers of preserved calcareous pelagic tests, thus markedly enhancing the proportion of siliceous pelagic tests, debris, and terrigenous and/or volcanic components. These phenomena might explain the high volcanic content in some abyssal plains, and illustrations of this on a more regional scale have been presented (Heath and Dymond, 1977). It would also help account for vertical lithofacies variations noted in the cores we examined, particularly *Lynch*-1.

This diagram (Figure 23), which models abyssal plain sedimentation, is largely idealized, and based on general concepts. We have indicated the approximate location of the southern Sohm Abyssal Plain cores on the theoretical plot. It is noted that even in an abyssal plain such as the Sohm, which has had ample and direct access to abundant terrigenous sources, particularly during the Pliocene and Quaternary, the volcanic fraction is significant. Although not dominant, this fraction may constitute as much as 1 percent, and locally up to 5 percent, of the total sediment fill. These values are modest when compared to the proportion of volcaniclastic sediments in regions close to volcanic arcs (Sigurdsson et al., 1980).

We predict that further detailed petrographic examination of cores collected in the Sohm and other abyssal plains will reveal that locally derived reworked material of both sedimentary and volcanic origin may account for a significant fraction of the total sediment fill of abyssal areas.

Appendix

Tables

TABLE 1.—Grain-size analyses from selected samples of cores studied, showing percentages of sand (>63 μm), silt, and clay (<2 μm) and also the silt/clay ratio (T = trace; dashed lines = not processed)

Sample depth(cm)	% sand	% silt	% clay	silt/clay ratio
ATLANTIS core 153-141				
7-8	T	50	50	1.00
49-50	T	77	23	3.34
109-110	T	62	38	1.63
172-173	T	32	68	0.47
212-213	T	35	65	0.53
240-241	T	31	69	0.44
265-266	T	88	12	7.33
327-328	T	38	62	0.61
384-385	5	78	17	4.58
400-401	56	34	10	3.40
465-466	68	26	6	4.33
500-501	67	24	9	2.66
575-580	67	26	7	3.71
660-661	24	37	39	0.94
720-721	51	31	18	1.72
745-746	36	37	27	1.37
807-809	65	28	7	4.00
923-924	65	27	8	3.37
985-986	67	33	T	>33.0
VEMA core 22-231				
0-2	T	37	68	0.54
11-13	2	35	65	0.53
85-87	T	36	64	0.56
122-123	T	30	70	0.52
168-170	T	28	72	0.38
245-247	T	36	64	0.56
253-255	T	37	63	0.58
401-403	T	72	28	2.57
498-500	T	60	40	1.50
672-673	T	38	62	0.61
681-683	T	48	52	0.92
913-915	T	49	51	0.96
927-929	T	46	54	0.85
1050-1052	T	58	42	1.38
1221-1223	T	73	27	2.70
1236-1237	T	51	49	1.04
1304-1305	42	40	18	2.22
1353-1354	T	78	22	3.54
1460-1462	T	37	63	0.58
1480-1481	T	62	38	1.63

Sample depth(cm)	% sand	% silt	% clay	silt/clay ratio
VEMA core 26-6				
2-3	4	35	61	0.57
29-32	T	34	66	0.51
45-47	T	29	71	0.40
124-126	T	25	75	0.33
227-229	T	20	80	0.25
272-274	T	21	79	0.26
321-323	1	19	80	0.23
344-346	3	27	70	0.38
393-395	T	17	83	0.20
474-476	T	27	73	0.36
544-546	T	18	82	0.21
VEMA core 26-9				
1-3	T	34	66	0.51
44-46	T	34	66	0.51
51-53	T	30	70	0.42
159-161	T	14	86	0.16
225-227	T	14	86	0.16
280-282	T	14	86	0.16
407-409	T	14	86	0.16
435-437	T	14	86	0.16
503-505	T	14	86	0.16
593-595	T	13	87	0.14
LYNCH core 710-78-1				
13-15	2	42	56	0.75
34-36	T	35	65	0.53
80-82	T	37	63	0.58
195-197	T	52	48	1.08
225-227	T	73	27	2.70
297-299	4	--	--	--
299-301	10	--	--	--
301-303	50	25	25	1.0
304-306	3	--	--	--
345-347	T	42	58	0.72
372-375	1	55	44	1.25
434-436	T	32	68	0.47
443-445	T	72	28	2.57
542-544	1	46	55	0.83
557-559	3	51	46	1.10

TABLE 2.—Summary of results of grain-size and compositional analyses of core *Atlantis* 153-141, depth 5350 m

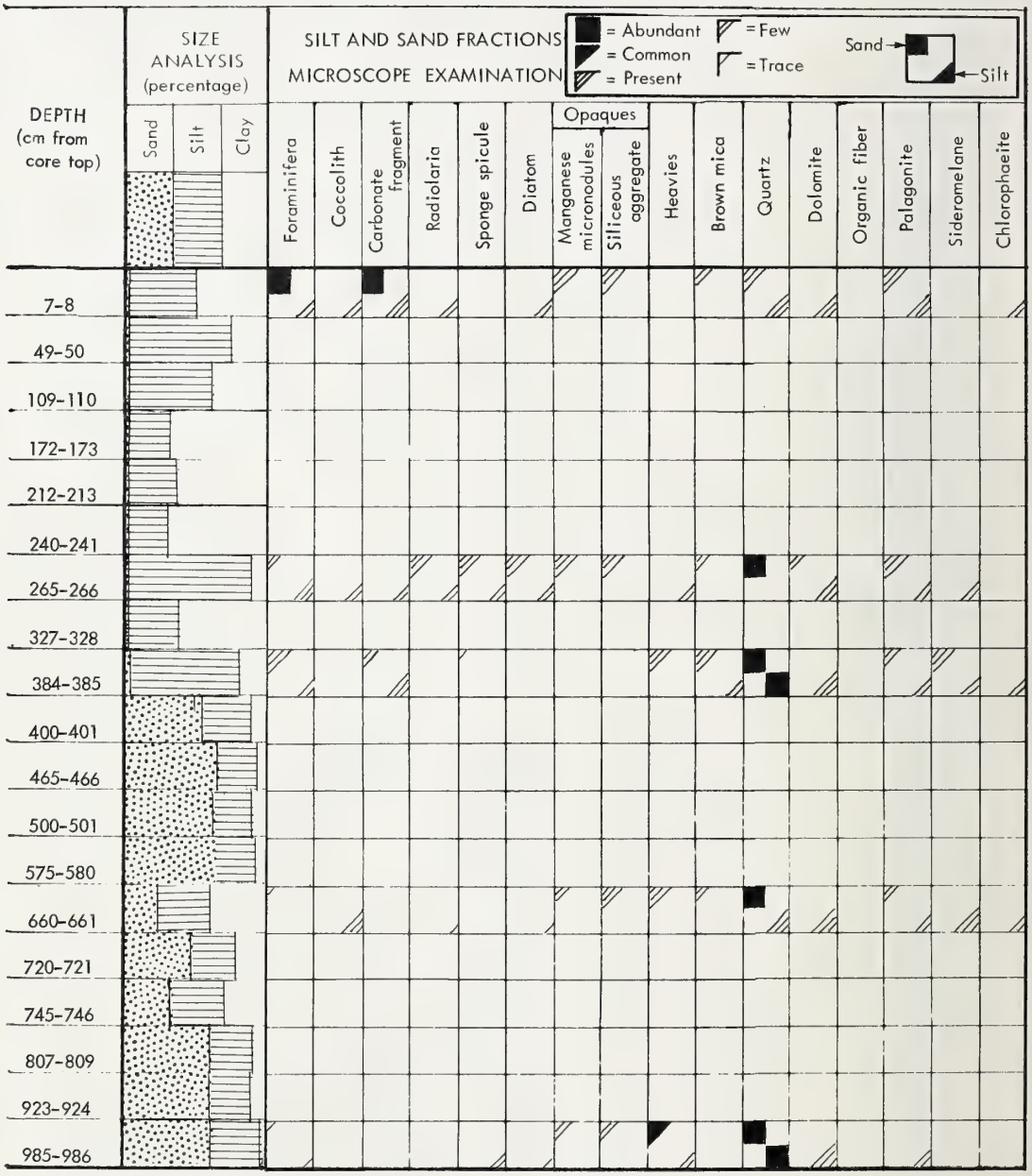

TABLE 2.—Continued

CLAY-SIZE FRACTION X-RAY DIFFRACTION (percentage)									SILT-SIZE FRACTION X-RAY DIFFRACTION (percentage)								Manganese, fluorescence (as counts/0.1 mg/200 sec)	REMARKS
Montmorillonite	Mica	Kaolinite plus Chlorite	Amphibole	Quartz	K feldspar	Plagioclase	Calcite	Dolomite	Mica	Kaolinite plus Chlorite	Amphibole	Quartz	K feldspar	Plagioclase	Calcite	Dolomite		
T	42	33			8	9	8		8	8	2	7	7	23	20	25	5.9	Few aggregates are iron cemented, some are dark red; inorganic crystalline calcite and feldspar present.
									5	2	T	5	7	29	24	28		
																	7.8	
									18	20	1	10	5	15	16	15		
T	63	37															6.8	
																		Inorganic crystalline calcite abundant; silt is coarse-grained.
									15	23		8	4	15	20	15	3.2	
T	46	40			5	9			3	3	T	11	24	29	10	20		Terrigenous sand with abundant feldspar and with inorganic crystalline calcite; silt is poorly sorted.
																	4.6	
T	55	34			4	5	2		6	8	T	8	10	28	11	29	5.2	Same as above.
									4	5	2	7	14	32	11	25	6.0	
	62	38					T		3	3	1	13	17		12	18	5.2	Same as above.

TABLE 3.—Summary of results of grain-size and compositional analyses of core *Vema* 22-231, depth 5535 m

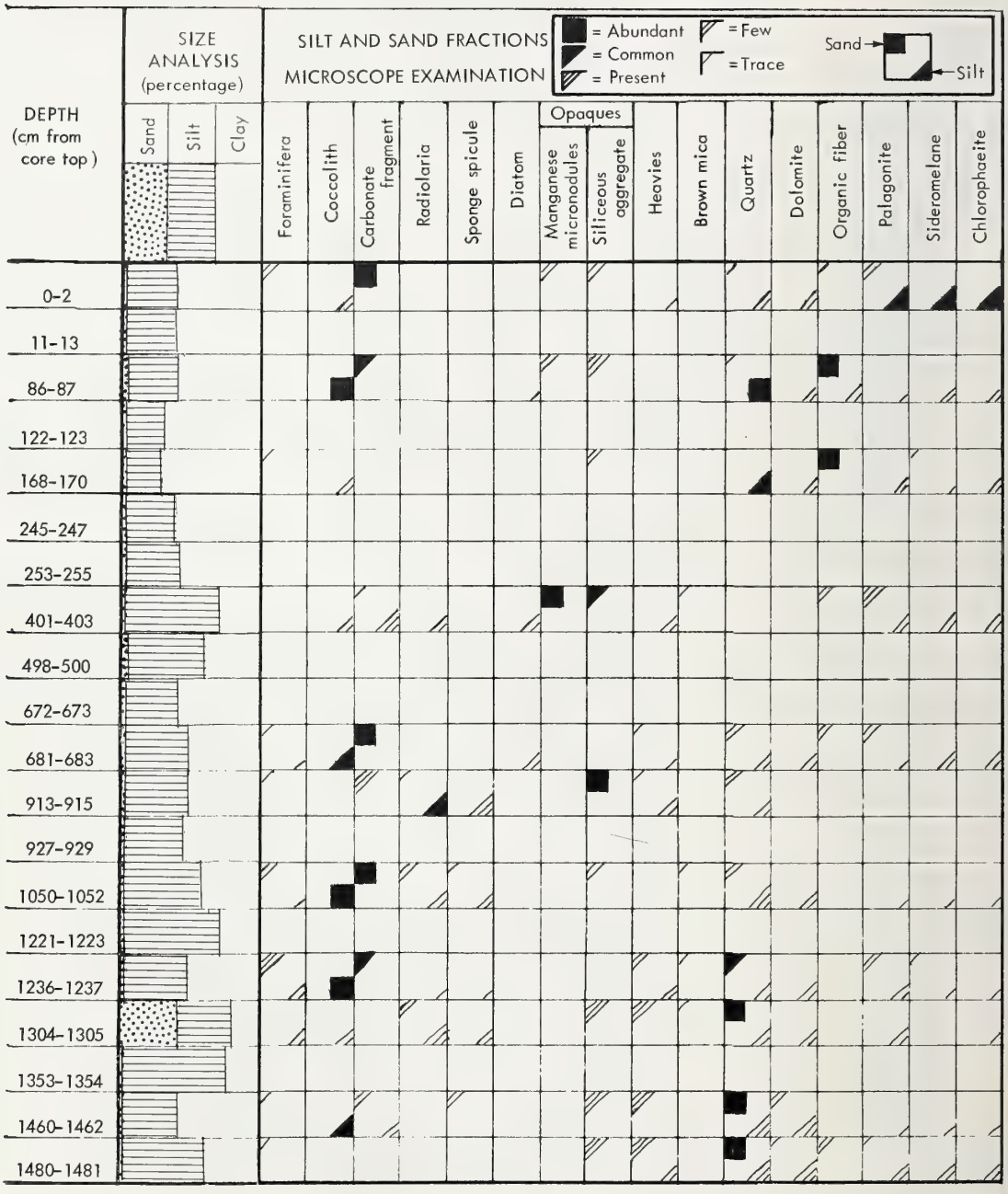

TABLE 3.—Continued

CLAY-SIZE FRACTION X-RAY DIFFRACTION (percentage)									SILT-SIZE FRACTION X-RAY DIFFRACTION (percentage)								Manganese, fluorescence (as counts/0.1 mg/200 sec)	REMARKS
Montmorillonite	Mica	Kaolinite plus Chlorite	Amphibole	Quartz	K feldspar	Plagioclase	Calcite	Dolomite	Mica	Kaolinite plus Chlorite	Amphibole	Quartz	K feldspar	Plagioclase	Calcite	Dolomite		
									14	17	2	7	5	16	15	24	7.3	Most aggregates are iron stained; some manganese droplets are oxidized.
T	42	33			T	T	25		6	4	4	4	7	18	26	31	8.1	Siliceous aggregates are light brown.
									21	25	1	14	3	12	12	12		
T	53	47			T	T												
																	10.0	Siliceous aggregates are gold colored; silt grains are unusually large.
									6	6	1	7	11	27	12	30		
									8	7	2	5	4	20	32	22		
									8	11	1	9	5	18	18	30	6.2	Inorganic crystalline calcite grains are chemically etched.
T	52	41	7			T			15	19	3	10	7	17	4	29		Aggregates are light brown or white; silt is coarse-grained; one grain of garnet.
																	8.6	Aggregates are white and occasionally light brown; inorganic crystalline calcite noted.
T	49	51				T	T		8	9	T	12	8	23	15	22		
																		Garnet is present.
																	8.5	Terrigenous sand, poorly sorted.
									7	7	1	11	7	22	20	25		
T	41	20			6	11	22	T	10	9	1	7	3	13	34	23		Terrigenous sand, poorly sorted.
									24	15	2	13	7	24		15	7.6	Terrigenous sand, poorly sorted, with garnet; aggregates are iron stained.

TABLE 4.—Summary of results of grain-size and compositional analyses of cores *Vema* 26-6, depth 5207 m, and 26-9, depth 5546 m

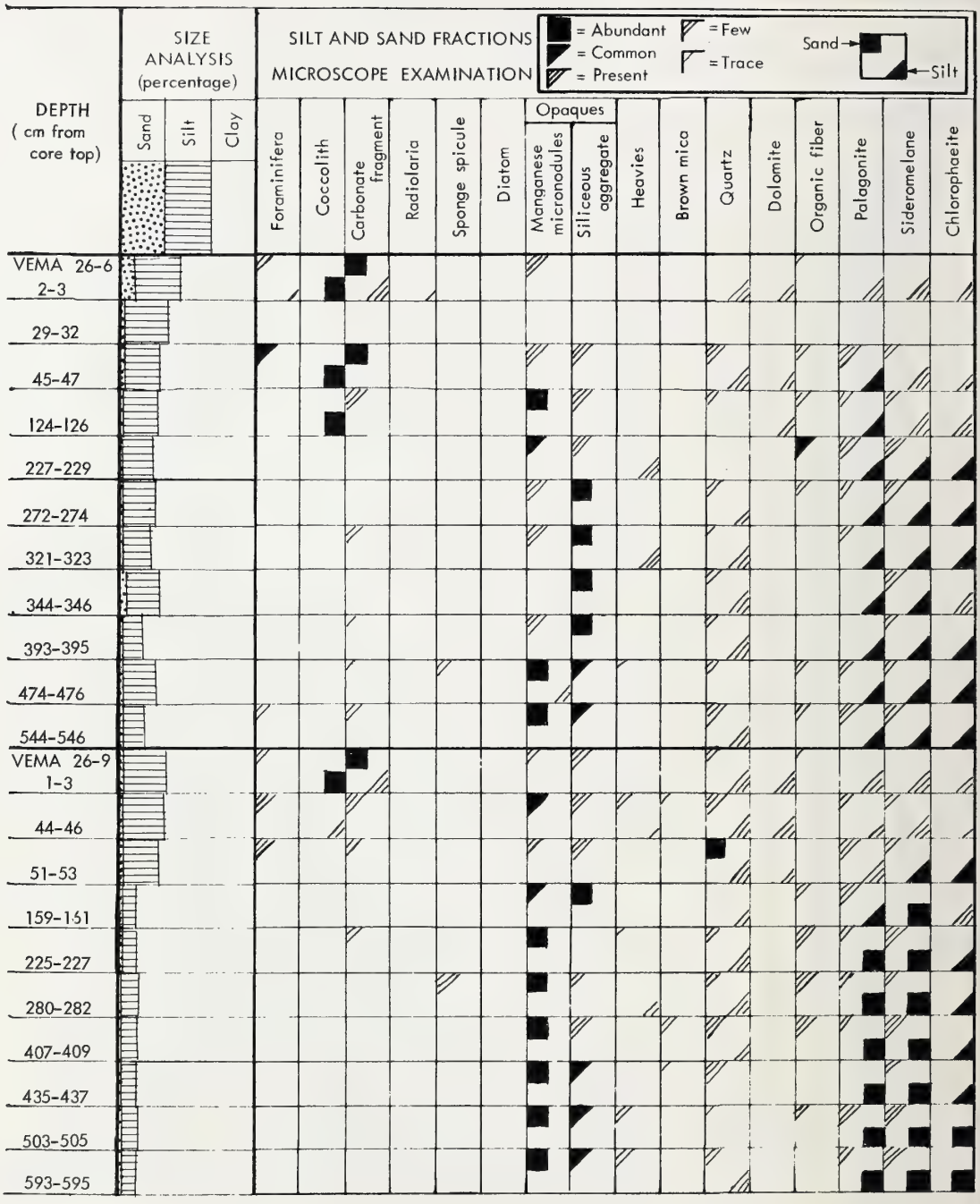

TABLE 4.—Continued

CLAY-SIZE FRACTION X-RAY DIFFRACTION (percentage)									SILT-SIZE FRACTION X-RAY DIFFRACTION (percentage)								Manganese, fluorescence (as counts/0.1 mg/200 sec)	REMARKS
Montmorillonite	Mica	Kaolinite plus Chlorite	Amphibole	Quartz	K feldspar	Plagioclase	Calcite	Dolomite	Mica	Kaolinite plus Chlorite	Amphibole	Quartz	K feldspar	Plagioclase	Calcite	Dolomite		
	18	23				10	49		10	13	T	5	3	12	47	8	9.7	Large platy iron fragments.
																	7.1	
28	13	21		5			33										26.3	
40	26	28				T	7		16	17	2	13	8	22	13	9	31.5	Inorganic crystalline calcite; weathered glass with abundant inclusions.
44	29	27							23	25	3	14	11	24			37.1	Aggregates are iron stained; some weathered glass; rod-shaped silt crystals probably pyroxenes.
35	25	26			4	10			19	20	2	17	12	30			37.4	Few feldspar grains.
37	12	45		6	T	T			18	26		15	9	32			54.9	Few feldspar grains; these and other sand grains are rounded to subrounded.
25	21	54							16	36		9	20	19			34.9	Few feldspar grains; silt poorly sorted.
37	18	45		T		T			6	35	2	9	18	30			60.9	Few feldspar grains.
52	14	34							5	43		5	19	28			58.9	Few feldspar grains; silt poorly sorted with rod-shaped grains.
28	28	44				T			14	23		9	34	20			49.5	Few feldspar grains; silt is coarse-grained.
T	39	39					22		15	15	1	11	6	12	19	21	8.3	Aggregates are occasionally iron stained; inorganic crystalline calcite in silt.
7	46	29		4	5	9			18	14	5	11	8	20		24	12.3	Few feldspar grains; silt, poorly sorted, with rod-shaped grains.
25	38	28			4	5			15	15	4	11	8	22		25	12.8	Few feldspar grains; rod-shaped grains in the silt fraction.
39	26	25							25	23		13	14	25			20.7	Siliceous aggregates were originally brown glass.
28	20	52			T				28	24		13	13	22			17.4	Weathered glass present.
27	16	57		T					23	26		13	13	20			23.8	Feldspar and weathered glass present.
26	31	43							23	26		13	18	20			29.5	Few aggregates are iron cemented; few feldspar grains.
30	23	47							23	20		11	17	29			25.8	Few feldspar grains; weathered glass present; rod-shaped grains in silt.
29	19	52							21	29		11	16	23			29.1	Aggregates are iron stained; rod-shaped grains in silt fraction.
46	9	45							16	30		20	25	9			32.5	Aggregates are white or red; few feldspar grains; rod-shaped grains in silt fraction.

TABLE 5.—Summary of results of grain-size and compositional analyses of core *Lynch* 710-78-1, depth 5207 m

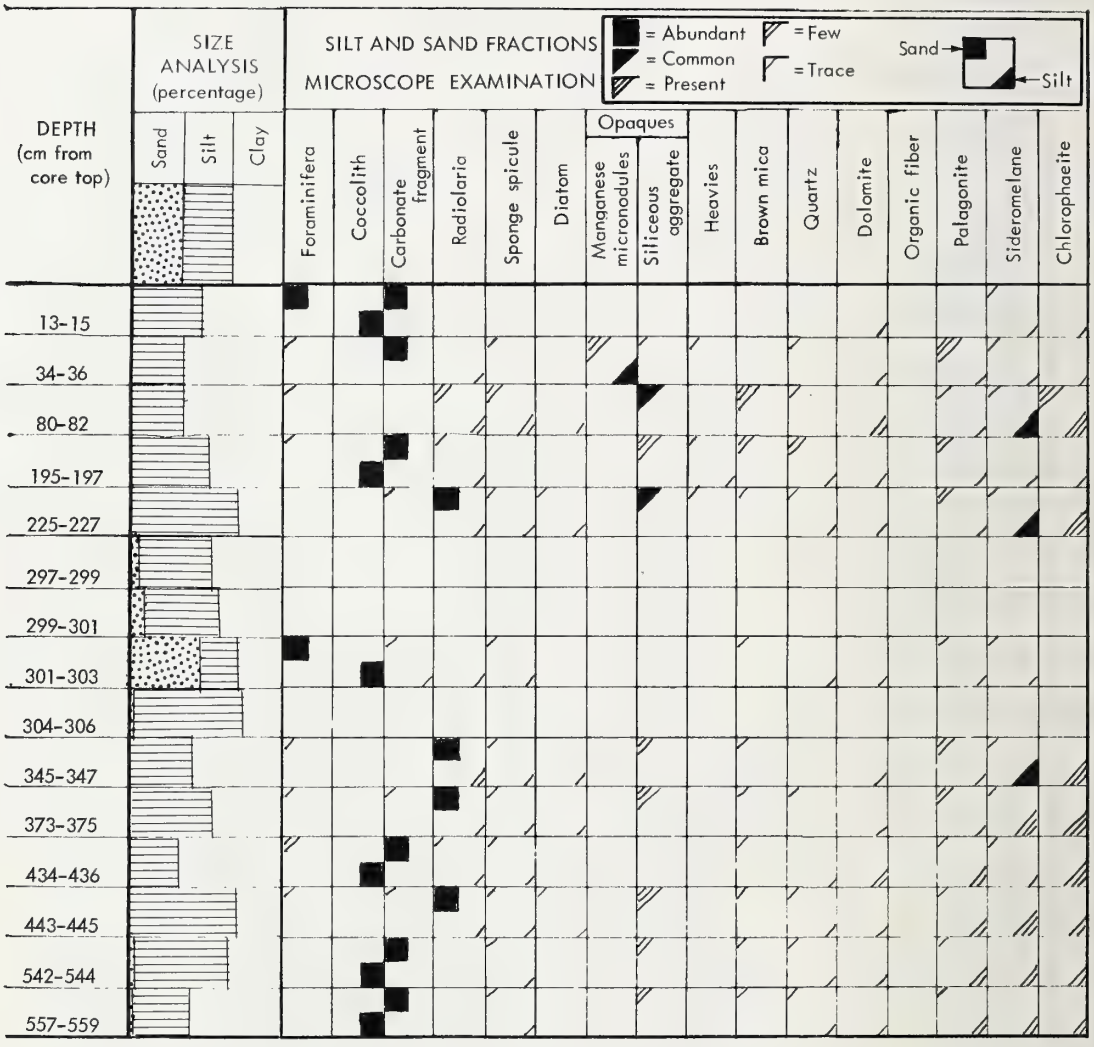

TABLE 5.—Continued

CLAY-SIZE FRACTION X-RAY DIFFRACTION (percentage)									SILT-SIZE FRACTION X-RAY DIFFRACTION (percentage)								Manganese, fluorescence (as counts/0.1 mg/200 sec)	REMARKS
Montmorillonite	Mica	Kaolinite plus Chlorite	Amphibole	Quartz	K feldspar	Plagioclase	Calcite	Dolomite	Mica	Kaolinite plus Chlorite	Amphibole	Quartz	K feldspar	Plagioclase	Calcite	Dolomite		
17	20	28		5	2	4	24		1	16		9	3	11	38	12	3630	Few foraminifera tests are iron stained; ash is devitrified.
14	47	30		2	1	2	4		26	31		10	4	12	T	17	1890	All foraminifera tests and quartz grains are iron stained.
15	53	18		3	1	4			22	38		14	3	14		9	1890	Abundant devitrified glass.
10	42	30		2	2	4	8	2	16	15		11	4	17	16	21	3310	Feldspar and large quartz grains.
8	54	33		2		4			14	13		8	3	14		48	2800	Foraminifera fragments are ironstained; hornblende.
6	29	17				5	42		7	7		7	T	12	55	12	3110	
14	30	41		5	3	7			21	16		14	6	21		22	2350	Few foraminifera fragments are iron stained.
15	49	30			1	5			18	19		17	6	23		17	2580	
12	46	30		2	2	3	5	T	25	22		9	3	10	7	14	3470	
13	35	36			4	2			20	20		23	7	18		12	1840	All foraminifera fragments are iron stained.
15	39	24		4		4	15		15	12		9	3	15	29	17	4200	
9	15	16			2	7	51		7	6		5	3	13	56	10	4620	

Literature Cited

Amos, A. F., and R. D. Gerard
1979. Anomalous Bottom Water South of the Grand Banks Suggests Turbidity Current Activity. *Science*, 203:894–897.

Arrhenius, G.
1963. Pelagic Sediments. *In* M. N. Hill, editor, *The Sea*, 3:655–727. London: Interscience Publishers.

Biscaye, P. E.
1965. Mineralogy and Sedimentation of Recent Deep-Sea Clay in the Atlantic Ocean and Adjacent Seas and Oceans. *Geological Society of America Bulletin*, 76: 803–832.

Biscaye, P. E., and S. E. Eittreim
1977. Suspended Particulate Loads and Transports in the Nepheloid Layer on the Abyssal Atlantic Ocean. *Marine Geology*, 23:155–172.

Bowles, F. A.
1980. Stratigraphy and Sedimentation of the Archipelagic Apron and Adjoining Area Southeast of Bermuda. *Marine Geology*, 37:267–294.

Brown, N. L.
1974. A Precision CTD Microprofiler. *Institute of Electrical and Electronic Engineers International Conference on Engineering in the Ocean Environment*, 2:270–278.

CLIMAP project members
1976. The Surface of the Ice-Age Earth. *Science*, 191: 1131–1137.

Duplessy, J.-C., J. Moyers, and C. Pujol
1980. Deep Water Formation in the North Atlantic Ocean during the Last Ice Age. *Nature*, 286:479–482.

Ericson, D. B., M. Ewing, G. Wollin, and B. C. Heezen
1961. Atlantic Deep-Sea Sediment Cores. *Geological Society of America Bulletin*, 72:193–286.

Ewing, J., M. Ewing, C. Windisch, and T. Aiken
1974. Seismic Reflection Profiles. In *Underway Marine Geophysical Data in the North Atlantic—June 1961–January 1971*, part E. Palisades, New York: Lamont-Doherty Geological Observatory of Columbia University.

Ewing, M., G. Carpenter, C. Windisch, and J. Ewing
1973. Sediment Distribution in the Oceans: The Atlantic. *Geological Society of America Bulletin*, 84:71–88.

Fox, P. J., A. M. Harrian, B. C. Heezen, W. Prell, and W.B.F. Ryan
1967. Contour Currents and Their Effect on the Distribution of Sediment on the Northern Bermuda Rise [Abstract]. *Program of the Annual Meeting in New Orleans, Geological Society of America*, 1967:70–71.

Fox, P. J., and B. C. Heezen
1965. Sands of the Mid-Atlantic Ridge. *Science*, 149: 1367–1370.

Furnes, H.
1980. Chemical Changes during Palagonitization of an Alkaline Olivine Basaltic Hyaloclastite, Santa Maria, Azores. *Neues Jahrbuch für Mineralogie*, 138: 14–30.

Heath, G. R., and J. Dymond
1977. Genesis and Transformation of Metalliferous Sediments from the East Pacific Rise, Bauer Deep, and Central Basin, Northwest Nazca Plate. *Geological Society of America Bulletin*, 88:723–733.

Heezen, B. C.
1963. Turbidity Currents. *In* M. N. Hill, editor, *The Sea*, 3:742–775. London: Interscience Publishers.

Heezen, B. C., and M. Ewing
1952. Turbidity Currents and Submarine Slumps and the Grand Banks Earthquake. *American Journal of Science*, 250:849–873.

Heezen, B. C., and C. D. Hollister
1971. *The Face of the Deep.* 659 pages, illustrated. New York: Oxford University Press.

Heezen, B. C., and A. S. Laughton
1963. Abyssal Plains. *In* M. N. Hill, editor, *The Sea*, 3: 312–364. London: Interscience Publishers.

Heezen, B. C., and M. Tharp
1968. *The Floor of the Oceans* [chart]. New York: Geological Society of America.

Heezen, B. C., M. Tharp, and M. Ewing
1959. The Floors of the Oceans—the North Atlantic. *Geological Society of America Special Paper*, 65: 122 pages.

Honnorez, J.
1978. Generation of Phillipsites by Palagonitization of Basaltic Glass in Sea Water and the Origin of K-rich Deep-Sea Sediments. *In* L. B. Sand and F. A. Mumpton, editors, *Natural Zeolites: Occurrence, Properties, Use,* pages 245–258. Oxford: Pergamon Press.

Horn, D. R., M. Ewing, B. M. Horn, and M. N. Delach
1971. Turbidites of the Hatteras and Sohm Abyssal Plains, Western North Atlantic. *Marine Geology*, 11: 287–323.

Houtz, R. E.
1974. Preliminary Study of Global Sediment Sound Velocities from Sonobouy Data. *In* L. Hampton, editor, *Physics of Sound in Marine Sediments*, pages 519–534. New York: Plenum Publishing Corporation.

Huang, T. C.
1980. A Volcanic Sedimentation Model: Implications of Processes and Responses of Deep-Sea Ashes. *Marine Geology*, 38:103–122.

Huang, T. C., N. D. Watkins, and D. M. Shaw
1975. Atmospherically Transported Volcanic Glass in Deep-Sea Sediments: Development of a Separation and Counting Technique. *Deep Sea Research*, 22:185–196.

Huang, T. C., N. D. Watkins, and L. Wilson
1979. Deep-Sea Tephra from the Azores during the Past 300,000 Years: Eruptive Cloud Height and Ash Volume Estimates. *Geological Society of America Bulletin*, 90:235–288.

Hubert, J. F.
1964. Textural Evidence for Deposition of Many Western North Atlantic Deep-Sea Sands by Ocean-Bottom Currents Rather Than Turbidity Currents. *The Journal of Geology*, 72:757–785.

Jansa, L. F., P. Enos, B. E. Tucholke, F. M. Gradstein, and R. E. Sheridan
1979. Mesozoic-Cenozoic Sedimentary Formation of the North American Basin; Western North Atlantic. *In* M. Talwani, W. Hay, and W.B.F. Ryan, editors, Deep Drilling Results in the Atlantic Ocean: Continental Margins and Paleoenvironment. *Maurice Ewing Series*, 3:3–57. Washington: American Geophysical Union.

Laine, E. P.
1978. Geological Effects of the Gulf Stream System in the North American Basin. 164 pages. Doctoral dissertation, Woods Hole Oceanographic Institution–MIT.

Laine, E. P., and C. D. Hollister
1981. Geological Effects of the Gulf Stream System on the Northern Bermuda Rise. *Marine Geology*, 39: 277–310.

LaTouche, C., and M. Parra
1979. La Sédimentation au Quaternaire Recent dans le "Northwest Atlantic Mid-Ocean Canyon"—Apport des données minéralogiques et géochimiques. *Marine Geology*, 29:137–164.

Nayudu, Y. R.
1971. Geologic Implications of Microfossils in Submarine Volcanics. *Bulletin Volcanologique*, 35:402–423.

Peacock, M., and R. Fuller
1928. Chlorophaeite, Sideromelane and Palagonite from the Columbia River Plateau. *The American Mineralogist*, 13:360–382.

Peterson, M.N.A., N. T. Edgar, C. van der Borch, M. B. Cita, S. Gartner, Jr., R. Goll, and C. Nigrini
1970. Site 9. *In* M.N.A. Peterson, N. T. Edgar, M. B. Cita, S. Gartner, Jr., R. Goll, and C. van der Borch, editors, *Initial Reports of the Deep Sea Drilling Project*, 2:35–116. Washington: U.S. Government Printing Office.

Pilkey, O. H., S. D. Locker, and W. J. Cleary
1980. Comparison of Sand Layer Geometry on Flat Floors of 10 Modern Depositional Basins. *The American Association of Petroleum Geologists Bulletin*, 64:841–856.

Ruddiman, W. F.
1977. North Atlantic Ice Rafting: A Major Change at 75,000 Years before the Present. *Science*, 196:1208–1210.

Ruddiman, W. F., and A. McIntyre
1976. Northeast Atlantic Paleoclimatic Changes over the Past 600,000 Years. *Geological Society of America Memoir*, 145:111–146. Boulder, Colorado: Geological Society of America.
1979. Warmth of the Subpolar North Atlantic Ocean during Northern Hemisphere Ice-Sheet Growth. *Science*, 204:173–175.

Schmitz, W. J., Jr.
1977. On the Deep General Circulation in the Western North Atlantic. *Journal Marine Research*, 35:21–28.

Schnitker, D.
1974. West Atlantic Abyssal Circulation during the Past 120,000 Years. *Nature*, 248:385–387.
1979. The Deep Waters of the Western North Atlantic during the Past 24,000 Years, and the Re-initiation of the Western Boundary Undercurrent. *Marine Micropaleontology*, 4:265–280.

Scott, M. R., P. F. Salter, and L. A. Barnard
1979. Chemistry of Ridge-Crest Sediments from the Northern Atlantic Ocean. *In* M. Talwani, C. G. A. Harrison, and D. E. Hayes, editors, Deep Drilling Results in the Atlantic Ocean: Ocean Crust. *Maurice Ewing Series*, 2:403–428. Washington: American Geophysical Union.

Siever, R., and M. Kastner
1967. Mineralogy and Petrology of Some Mid-Atlantic Ridge Sediments. *Journal of Marine Research*, 25: 263–287.

Sigurdsson, H., R.S.J. Sparks, S. N. Carey, and T. C. Huang
1980. Volcanogenic Sedimentation in the Lesser Antilles Arc. *Journal of Geology*, 88:523–540.

Silva, A. J., C. D. Hollister, E. P. Laine, and B. E. Beverly
1976. Geotechnical Properties of Deep-Sea Sediments: Bermuda Rise. *Marine Geotechnology*, 1:195–232.

Stanley, D. J., and P. T. Taylor
1977. Sediment Transport down a Seamount Flank by a Combined Current and Gravity Process. *Marine Geology*, 23:77–88.

Stonecipher, S.
1978. Chemistry and Deep-Sea Phillipsite, Clinoptilolite, and Host Sediments. *In* L. B. Sand and F. A. Mumpton, editors, *Natural Zeolites: Occurrence, Properties, Use*, pages 221–234. Oxford: Pergamon Press.

Taylor, P. T., and R. Hekinian
1971. Geology of a Newly Discovered Seamount in the New England Seamount Chain. *Earth and Planetary Science Letters*, 11:73–82.

Thiede, J., T. Agdestein, and J. E. Strand
1980. Depth Distribution of Calcareous Sediments in the Mesozoic and Cenozoic North Atlantic Ocean. *Earth and Planetary Science Letters*, 47:416–422.

Tucholke, B. E., and G. S. Mountain
1979. Seismic Stratigraphy, Lithostratigraphy and Paleosedimentation Patterns in the North American Basin. *In* M. Talwani, C.G.A. Harrison, and D. E. Hayes, editors, Deep Drilling Results in the Atlantic Ocean: Ocean Crust. *Maurice Ewing Series*, 2: 58–86. Washington: American Geophysical Union.

Tucholke, B. E., and P. R. Vogt
1979. Site 382: Nashville Seamount—Volcanism along the Eastern New England Seamount Chain. *In* B. E. Tucholke, P. R. Vogt, I. O. Murdmaa, P. Rothe, R. L. Houghton, J. S. Galehouse, A. Kaneps, C. L. McNulty, Jr., H. Okada, J. W. Kendrick, K. R. Demars, and I. N. McCave, editors, *Initial Reports of the Deep-Sea Drilling Project*, 43:31–93. Washington: U.S. Government Printing Office.

Van Andel, T. H., and P. D. Komar
1969. Ponded Sediments of the Mid-Atlantic Ridge between 22° and 23° North Latitude. *Geological Society of America Bulletin*, 80:1163–1190.

Worthington, L. V.
1976. On the North Atlantic Circulation. *Johns Hopkins Oceanographic Studies*, 6: 110 pages. Baltimore: Johns Hopkins University Press.

Worzel, J. L.
1959. Extensive Deep Sea Subbottom Reflections Identified as White Ash. *Proceedings of the National Academy of Science*, 45:349–355.

Wüst, G.
1949. Blockdiagrame der Atlantischen Zirkulation auf Grund der "Meteor." *Ergebnisse Kieler Meeresforschungen*, 7, fig. 1. Kiel: Institut für Meereskunde der Universität Kiel.

REQUIREMENTS FOR SMITHSONIAN SERIES PUBLICATION

Manuscripts intended for series publication receive substantive review within their originating Smithsonian museums or offices and are submitted to the Smithsonian Institution Press with approval of the appropriate museum authority on Form SI–36. Requests for special treatment—use of color, foldouts, casebound covers, etc.—require, on the same form, the added approval of designated committees or museum directors.

Review of manuscripts and art by the Press for requirements of series format and style, completeness and clarity of copy, and arrangement of all material, as outlined below, will govern, within the judgment of the Press, acceptance or rejection of the manuscripts and art.

Copy must be typewritten, double-spaced, on one side of standard white bond paper, with 1¼" margins, submitted as ribbon copy (not carbon or xerox), in loose sheets (not stapled or bound), and accompanied by original art. Minimum acceptable length is 30 pages.

Front matter (preceding the text) should include: **title page** with only title and author and no other information, **abstract page** with author/title/series/etc., following the established format, **table of contents** with indents reflecting the heads and structure of the paper.

First page of text should carry the title and author at the top of the page and an unnumbered footnote at the bottom consisting of author's name and professional mailing address.

Center heads of whatever level should be typed with initial caps of major words, with extra space above and below the head, but with no other preparation (such as all caps or underline). Run-in paragraph heads should use period/dashes or colons as necessary.

Tabulations within text (lists of data, often in parallel columns) can be typed on the text page where they occur, but they should not contain rules or formal, numbered table heads.

Formal tables (numbered, with table heads, boxheads, stubs, rules) should be submitted as camera copy, but the author must contact the series section of the Press for editorial attention and preparation assistance before final typing of this matter.

Taxonomic keys in natural history papers should use the alined-couplet form in the zoology and paleobiology series and the multi-level indent form in the botany series. If cross-referencing is required between key and text, do not include page references within the key, but number the keyed-out taxa with their corresponding heads in the text.

Synonymy in the zoology and paleobiology series must use the short form (taxon, author, year:page), with a full reference at the end of the paper under "Literature Cited." For the botany series, the long form (taxon, author, abbreviated journal or book title, volume, page, year, with no reference in the "Literature Cited") is optional.

Footnotes, when few in number, whether annotative or bibliographic, should be typed at the bottom of the text page on which the reference occurs. Extensive notes must appear at the end of the text in a notes section. If bibliographic footnotes are required, use the short form (author/brief title/page) with the full reference in the bibliography.

Text-reference system (author/year/page within the text, with the full reference in a "Literature Cited" at the end of the text) must be used in place of bibliographic footnotes in all scientific series and is strongly recommended in the history and technology series: "(Jones, 1910:122)" or ". . . Jones (1910:122)."

Bibliography, depending upon use, is termed "References," "Selected References," or "Literature Cited." Spell out book, journal, and article titles, using initial caps in all major words. For capitalization of titles in foreign languages, follow the national practice of each language. Underline (for italics) book and journal titles. Use the colon-parentheses system for volume/number/page citations: "10(2):5–9." For alinement and arrangement of elements, follow the format of the series for which the manuscript is intended.

Legends for illustrations must not be attached to the art nor included within the text but must be submitted at the end of the manuscript—with as many legends typed, double-spaced, to a page as convenient.

Illustrations must not be included within the manuscript but must be submitted separately as original art (not copies). All illustrations (photographs, line drawings, maps, etc.) can be intermixed throughout the printed text. They should be termed **Figures** and should be numbered consecutively. If several "figures" are treated as components of a single larger figure, they should be designated by lowercase italic letters (underlined in copy) on the illustration, in the legend, and in text references: "Figure 9b." If illustrations are intended to be printed separately on coated stock following the text, they should be termed **Plates** and any components should be lettered as in figures: "Plate 9b." Keys to any symbols within an illustration should appear on the art and not in the legend.

A few points of style: (1) Do not use periods after such abbreviations as "mm, ft, yds, USNM, NNE, AM, BC." (2) Use hyphens in spelled-out fractions: "two-thirds." (3) Spell out numbers "one" through "nine" in expository text, but use numerals in all other cases if possible. (4) Use the metric system of measurement, where possible, instead of the English system. (5) Use the decimal system, where possible, in place of fractions. (6) Use day/month/year sequence for dates: "9 April 1976." (7) For months in tabular listings or data sections, use three-letter abbreviations with no periods: "Jan, Mar, Jun," etc.

Arrange and paginate sequentially EVERY sheet of manuscript—including ALL front matter and ALL legends, etc., at the back of the text—in the following order: (1) title page, (2) abstract, (3) table of contents, (4) foreword and/or preface, (5) text, (6) appendixes, (7) notes, (8) glossary, (9) bibliography, (10) index, (11) legends.